JYX JYVÄSKYLÄN YLIOPISTO UNIVERSITY OF JYVÄSKYLÄ

This is a self-archived version of an original article. This version may differ from the original in pagination and typographic details.

Author(s): ALICE collaboration

Title: Measurement of beauty production via non-prompt D0 mesons in Pb-Pb collisions at √sNN = 5.02 TeV

Year: 2022

Version: Published version

Copyright: © CERN, for the benefit of the ALICE Collaboration. Article funded by SCOAP3.

Rights: CC BY 4.0

Rights url: https://creativecommons.org/licenses/by/4.0/

Please cite the original version:

ALICE collaboration. (2022). Measurement of beauty production via non-prompt D0 mesons in Pb-Pb collisions at √sNN = 5.02 TeV. Journal of High Energy Physics, 2022(12), Article 126. https://doi.org/10.1007/JHEP12(2022)126

Published for SISSA by Springer

Received: September 26, 2022
Accepted: November 23, 2022
Published: December 21, 2022

Measurement of beauty production via non-prompt D^0 mesons in Pb-Pb collisions at $\sqrt{s_{NN}} = 5.02$ TeV

ALICE

The ALICE collaboration

E-mail: ALICE-publications@cern.ch

Abstract: The production of non-prompt D^0 mesons from beauty-hadron decays was measured at midrapidity ($|y| < 0.5$) in Pb-Pb collisions at a nucleon-nucleon center-of-mass energy of $\sqrt{s_{NN}} = 5.02$ TeV with the ALICE experiment at the LHC. Their nuclear modification factor (R_{AA}), measured for the first time down to $p_T = 1$ GeV/c in the 0–10% and 30–50% centrality classes, indicates a significant suppression, up to a factor of about three, for $p_T > 5$ GeV/c in the 0–10% central Pb-Pb collisions. The data are described by models that include both collisional and radiative processes in the calculation of beauty-quark energy loss in the quark-gluon plasma, and quark recombination in addition to fragmentation as a hadronisation mechanism. The ratio of the non-prompt to prompt D^0-meson R_{AA} is larger than unity for $p_T > 4$ GeV/c in the 0–10% central Pb-Pb collisions, as predicted by models in which beauty quarks lose less energy than charm quarks in the quark-gluon plasma because of their larger mass.

Keywords: Heavy Ion Experiments, Heavy Quark Production, Quark Gluon Plasma

ArXiv ePrint: 2202.00815

Open Access, Copyright CERN,
for the benefit of the ALICE Collaboration.
Article funded by SCOAP^3.

https://doi.org/10.1007/JHEP12(2022)126

JHEP12(2022)126

Contents

1 Introduction 1

2 Experimental apparatus and data sample 3

3 Data analysis 4

4 Systematic uncertainties 6

5 Results 6

6 Conclusions 12

The ALICE collaboration 20

1 Introduction

The formation in ultra-relativistic collisions of heavy nuclei of a quark-gluon plasma (QGP), a state in which quarks and gluons are not confined into hadrons, is supported by several measurements at SPS, RHIC and LHC accelerators [1–9], and expected from quantum chromodynamics (QCD) on the lattice [10–13]. Heavy quarks (charm and beauty) are produced in hard-scattering processes occurring in the early stage of the collision. As the medium expands, they interact with its constituents via inelastic (gluon radiation) [14, 15] and elastic [16–18] flavour-conserving scatterings that modify their momentum towards equilibrium with the surrounding quarks and gluons. As a consequence, high-momentum charm and beauty quarks lose energy. This in-medium energy loss, which carries information on the medium properties and expansion, can be investigated by measuring the nuclear modification factor ($R_{\rm AA}$) of heavy-flavour hadrons. The $R_{\rm AA}$ is defined as the ratio of the transverse-momentum ($p_{\rm T}$)-differential production yields measured in a given centrality interval in nucleus-nucleus collisions ($\mathrm{d}N_{\rm AA}/\mathrm{d}p_{\rm T}$) to the cross section in proton-proton (pp) collisions ($\mathrm{d}\sigma_{\rm pp}/\mathrm{d}p_{\rm T}$) scaled by the average nuclear overlap function $\langle T_{\rm AA}\rangle$ [19, 20] in the considered centrality interval. In-medium energy loss of quarks and gluons implies a softening of the final-state hadron $p_{\rm T}$ spectrum resulting in $R_{\rm AA} < 1$ at intermediate and high $p_{\rm T}$. Several measurements in Au-Au collisions at RHIC and Pb-Pb collisions at the LHC evidence a substantial energy loss of charm and beauty quarks due to their interactions in the QGP [21–42]. The difference between the $R_{\rm AA}$ of heavy-flavour hadrons or their decay products and that of light hadrons, mostly originating from gluon and light-quark fragmentation, indicates that the amount of energy loss is sensitive to the colour-charge dependence of the strong interaction, as well as to the effects that depend on the parton mass [29, 43–45]. In particular, beauty quarks are expected to lose less energy than charm quarks. At high $p_{\rm T}$, where energy loss is caused mainly by radiative processes, this difference is expected to derive from the "dead-cone" effect, which suppresses gluon radiation off massive quarks at angles smaller than $m_{\rm Q}/E$ (with $m_{\rm Q}$ and E being the quark mass

JHEP12(2022)126

and energy, respectively) with respect to the quark direction [46–49], an effect directly observed in pp collisions at the LHC [50]. This expectation is supported by experimental data showing higher R_{AA} for beauty than charm signals, qualitatively in line with theoretical predictions [29, 39, 42, 44, 45, 51–55]. At low momenta, heavy-quark propagation through the medium is described as a diffusion process, occurring via multiple low-energy-transfer interactions, that also favours the participation of heavy quarks in the collective expansion of the system [56, 57]. Because of the larger mass, beauty quarks should diffuse less than charm quarks and have a longer relaxation time, which should increase linearly with the quark mass [58, 59]. Therefore, the comparison of charm and beauty R_{AA} provides a handle to constrain the modeling of the diffusion process.

Other effects are also relevant in nuclear collisions, namely cold-nuclear-matter (CNM) effects, that are present even without the formation of a QGP, and hadronisation effects. The main CNM effect at LHC energies is the modification of the parton distribution functions (PDF), in particular the reduction of the gluon PDF at small Bjorken-x values ("nuclear shadowing") that can cause a suppression of heavy-flavour production. At midrapidity, shadowing is expected to be relevant mainly at low p_{T} (below 2–3 GeV/c) and stronger for charm than beauty quarks, as suggested also from measurements performed in p-Pb collisions [28, 60–67]. In a high quark-density environment like the QGP, low-momentum heavy quarks may hadronise by recombining with other quarks in the medium [57, 68]. Such a "coalescence" mechanism can enhance the production of heavy-flavour baryons and of hadrons with strange quarks relative to non-strange B and D mesons [30, 57, 69–71] and it influences the p_{T} and azimuthal distributions of the produced heavy-flavour hadrons in a different way with respect to "vacuum-like" fragmentation. Several theoretical models need to include this mechanism to describe the measured R_{AA} and azimuthal anisotropy of D mesons [72–83]. Hadronisation and CNM effects complicate the determination of fundamental parameters, such as the spatial diffusion coefficient and charm-quark relaxation time, determined from open-charm measurements [84, 85].

The different impact of the aforementioned effects on beauty- and charm-hadron observables, ultimately due to the different quark masses, offers a handle to constrain these effects and understand heavy-quark diffusion in the medium. Moreover, as stated in ref. [84], from a theoretical point of view, beauty hadrons represent a cleaner probe of the QGP compared to charm hadrons, in terms of the implementation of both microscopic interactions and transport, and as a measure of coupling strength for quarks that are unlikely to reach thermalisation in the medium [86–89]. While several measurements of charm R_{AA} and azimuthal anisotropy have been performed down to low p_{T} [21, 22, 24, 25, 27, 31, 38, 41, 55], the experimental information is still poor for low-momentum beauty hadrons. Existing data on the production of B mesons [40], J/ψ from beauty decays [42, 44, 55], and single leptons from beauty decays [53, 54] are not sensitive to B mesons with p_{T} around the B-meson mass or lower (for the lepton case the correlation between the lepton and parent beauty-hadron p_{T} is very broad). This leaves unconstrained a kinetic window fundamental to explore the effects mentioned above.

In this paper, we report the measurement of the p_{T}-differential yield and the R_{AA} of D^0 mesons from beauty-hadron decays (referred to as non-prompt D^0 mesons) in Pb-

JHEP12(2022)126

Pb collisions at a center-of-mass energy per nucleon pair $\sqrt{s_{\rm NN}} = 5.02\,\text{TeV}$, for the first time down to $p_{\rm T} = 1\,\text{GeV}/c$ in central (0–10%) and semi-central (30–50%) collisions. This represents a significant extension of the previous measurement by CMS [39] that allows us to compute for the first time the $p_{\rm T}$-integrated yield of non-prompt $\rm D^0$ mesons. The non-prompt $\rm D^0$-meson $R_{\rm AA}$ is compared to that of prompt $\rm D^0$ mesons, which are produced in the hadronisation of charm quarks or from the decay of excited open-charm and charmonium states. In what follows, when mentioning a given hadron species we implicitly refer also to its antiparticle.

The paper is structured as follows. The experimental apparatus and data sample used for the analysis are briefly presented in section 2. The reconstruction of non-prompt $\rm D^0$ mesons and all corrections applied to the raw yield are presented in section 3. The estimation of systematic uncertainties is briefly discussed in section 4. The results are presented in section 5 and conclusions are drawn in section 6.

2 Experimental apparatus and data sample

The data were collected with the ALICE detector during the LHC Run 2 in 2018. A detailed description of the ALICE apparatus and of its performance can be found in refs. [90, 91]. The Time Projection Chamber (TPC) [92] is the main tracking device for the measurement of particle momenta. The Inner Tracking System (ITS) [93] is exploited for the reconstruction of the primary interaction vertex and of the secondary decay vertices of charm- and beauty-hadron decays. Particle identification (PID) is provided by the measurement of the specific energy loss $\mathrm{d}E/\mathrm{d}x$ in the TPC and of the flight time of charged particles from the interaction point to the Time-Of-Flight detector (TOF) [94]. These detectors, which cover the pseudorapidity interval $|\eta| < 0.9$ and full azimuthal angle, are enclosed in a large solenoidal magnet providing a uniform magnetic field of 0.5 T parallel to the LHC beam direction. The event triggers and offline selection criteria are defined in ref. [29]. About 1.0×10^8 and 8.5×10^7 events in the 0–10% and 30–50% centrality classes were selected for further analysis, corresponding to integrated luminosities ($L_{\rm int}$) of about $130\,\mu\text{b}^{-1}$ and $56\,\mu\text{b}^{-1}$, respectively [20].

The correction factors for the detector acceptance and the signal reconstruction and selection efficiency were obtained by means of Monte Carlo (MC) simulations. In order to describe the charged-particle multiplicity and detector occupancy, underlying Pb-Pb events at $\sqrt{s_{\rm NN}} = 5.02\,\text{TeV}$ were simulated with the HIJING v1.383 generator [95]. In order to enrich the simulation of prompt and non-prompt $\rm D^0$-meson signals, pp collisions containing a $\rm c\bar{c}$ or $\rm b\bar{b}$ pair in each event were simulated with the PYTHIA 8.243 event generator [96] and the particles originating from a charm or a beauty quark were embedded into the underlying Pb-Pb event. The $p_{\rm T}$ distribution of prompt D mesons in the MC simulation was weighted in order to match the shape measured in data for prompt $\rm D^0$ mesons, while, for non-prompt $\rm D^0$ mesons, the parent beauty-hadron $p_{\rm T}$ shape was weighted to match the shape given by model calculations [72, 97, 98]. The generated particles were transported through the apparatus, which was modelled in the simulation using the GEANT3 transport code [99].

JHEP12(2022)126

3 Data analysis

The D^0 mesons were reconstructed via the decay channel $D^0 \to K^-\pi^+$ with a branching ratio (BR) equal to $(3.950 \pm 0.031)\%$ [100]. The candidates were defined by combining pairs of tracks with opposite charge, each with $|\eta| < 0.8$, $p_T > 0.5$ (0.4) GeV/c for the 0–10% (30–50%) centrality class, a number of crossed TPC pad rows larger than 70 (out of 159), and a minimum number of two hits (out of six) in the ITS, with at least one in either of the two innermost layers, as the main selections.

To reduce the combinatorial background and separate the prompt and non-prompt contributions, a two-step machine-learning classification based on the Boosted Decision Tree (BDT) algorithm provided by the TMVA library [101] was utilised. Variables sensitive to the typical topology of the prompt and non-prompt decay vertices were chosen as input for the BDT algorithm, similarly to what is described in more detail in ref. [102]. Before the training, a $\pm 3\,\sigma$ selection around the expected mean $\mathrm{d}E/\mathrm{d}x$ in the TPC and time of flight in the TOF was applied to identify pions and kaons, where σ is the resolution on the measured quantities. The BDT algorithm was trained in each p_T interval, using samples of non-prompt and prompt D^0 mesons from the MC simulation, and a sample of background candidates with an invariant mass in the sidebands of the D^0-meson peak from the data. In the first step the BDT was trained to separate non-prompt and prompt D^0 mesons, while in the second step it was trained to separate non-prompt D^0 mesons and combinatorial background. By tuning the selection on the BDT outputs, the fraction of non-prompt D^0 can be varied from about 5% up to 90% maintaining a reliable signal extraction.

The raw yield was extracted in each p_T interval via a binned maximum-likelihood fit to the candidate invariant-mass distribution. The invariant-mass (M) distributions from which the raw yields with enhanced contribution of non-prompt D^0 mesons are extracted are reported in figure 1. The non-prompt D^0 enriched invariant-mass distributions were fitted with a function composed of a Gaussian term for the signal and an exponential function to describe the background shape. For transverse-momentum (p_T) intervals 2–6 GeV/c, a second-order polynomial function was used and below 2 GeV/c a third-order polynomial function was used to describe the background shape. The contribution of signal candidates that are present in the invariant-mass distribution with the wrong decay-particle mass assignment (reflection) was parameterised by fitting the simulated reflection invariant-mass distributions with a double Gaussian function, and it was included in the total fit function. The ratio between the reflections and the signal yields was taken from simulations. To improve the stability of the fits, the widths of the D^0-meson signal peaks were fixed to the values extracted from data samples dominated by prompt candidates, given the naturally larger abundance of prompt compared to non-prompt D^0 mesons.

The fraction of non-prompt D^0 mesons in the raw yield $f_{\text{non-prompt}}$ was estimated by sampling the raw yield at different values of the BDT output related to the candidate probability of being a non-prompt D^0 meson. In this way, a set of raw yields Y_{i} with different contributions of prompt and non-prompt D^0 was obtained. The Y_{i} can be related to the corrected yields of prompt (N_{prompt}) and non-prompt ($N_{\text{non-prompt}}$) D^0 mesons via the acceptance-times-efficiency (Acc $\times\, \epsilon$) factors as follows

$$(\mathrm{Acc} \times \epsilon)_{\mathrm{i}}^{\text{prompt}} \times N_{\text{prompt}} + (\mathrm{Acc} \times \epsilon)_{\mathrm{i}}^{\text{non-prompt}} \times N_{\text{non-prompt}} - Y_{\mathrm{i}} = \delta_{\mathrm{i}}. \tag{3.1}$$

JHEP12(2022)126

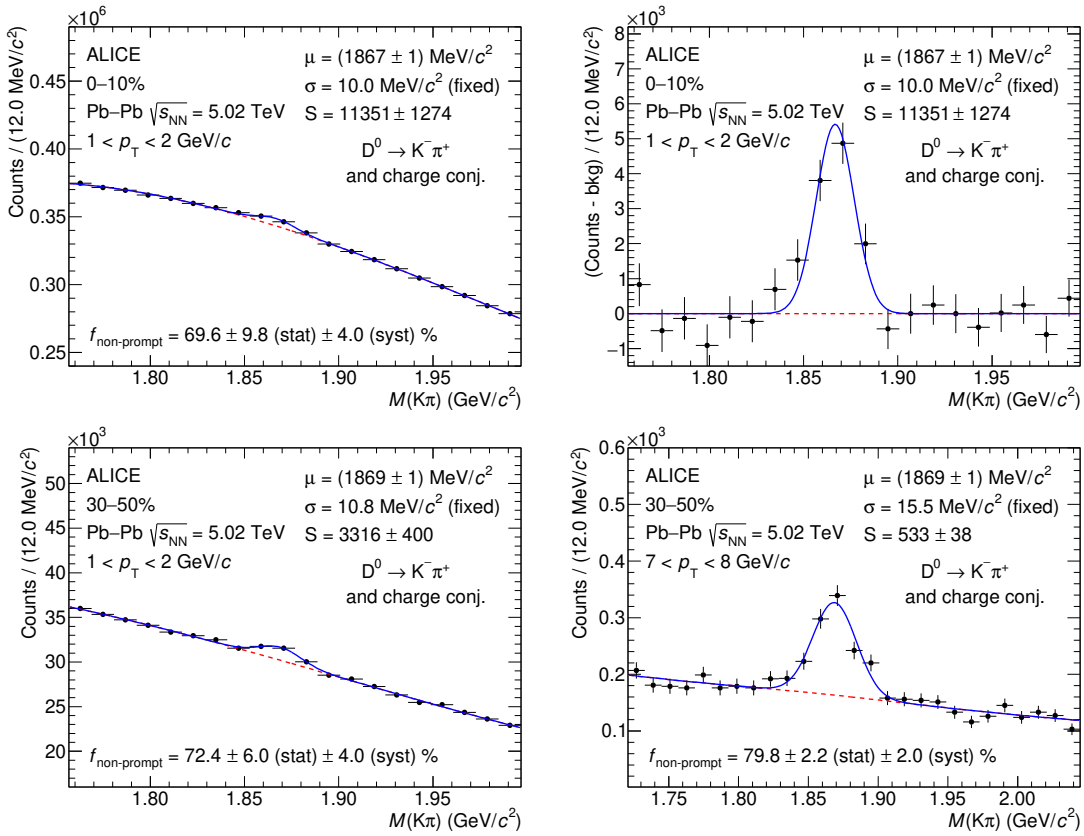

Figure 1. Invariant-mass distributions for D^0 candidates in selected p_T intervals for the centrality class 0–10% and 30–50%. Fitted values for the D^0 meson mass μ, width σ, and raw yield S are also given, the fraction of D^0 candidates in the measured raw yield is reported with its statistical and systematic uncertainties. Top row: non-prompt D^0 mesons with $1 < p_T < 2\,\mathrm{GeV}/c$ in the 0–10% centrality class, before (left) and after (right) subtraction of the background fit function. Bottom row: non-prompt D^0 mesons with $1 < p_T < 2\,\mathrm{GeV}/c$ (left) and $7 < p_T < 8\,\mathrm{GeV}/c$ (right) in the 30–50% centrality class.

In the above equation, δ_i represents a residual that accounts for the equation not holding exactly because of the uncertainties on Y_i, $(\mathrm{Acc} \times \epsilon)_i^{\text{non-prompt}}$, and $(\mathrm{Acc} \times \epsilon)_i^{\text{prompt}}$. With $n \geq 2$ sets, starting from eq. (3.1) a χ^2 function can be defined, which can be minimised to obtain N_{prompt} and $N_{\text{non-prompt}}$. More details can be found in ref. [102]. However, rather than using the $N_{\text{non-prompt}}$ parameter from the χ^2 minimisation, one of the n sets with a high non-prompt component was selected as a working point (wp), and $N_{\text{non-prompt}}$ and N_{prompt} were used to calculate the $f_{\text{non-prompt, wp}}$ fraction of the related raw yield Y_{wp}. This choice facilitates the estimate of systematic uncertainties. Then, to obtain the corrected non-prompt D^0-meson yield, the product $Y_{\text{wp}} \times f_{\text{non-prompt, wp}}$ was corrected for the corresponding acceptance-times-efficiency $(\mathrm{Acc} \times \epsilon)_{\text{wp}}^{\text{non-prompt}}$ and divided by a factor $2 \times \mathrm{BR} \times \Delta p_T \times \Delta y \times N_{\text{ev}}$, where Δp_T and Δy are the widths of the p_T and rapidity intervals, BR is the branching ratio of the decay channel, N_{ev} represents the number of analyzed events, and the factor 2 accounts for the fact that both particles and anti-particles are counted in the raw yield.

JHEP12(2022)126

4 Systematic uncertainties

Several sources of systematic uncertainties on the non-prompt D^0-meson corrected yields were studied. The systematic uncertainty on the raw yield extraction ranges from 4% to 14% depending on p_T and collision centrality class. It was evaluated by varying the lower and upper limits of the fit range, and the background fit function. The contribution due to the uncertainty on track reconstruction efficiency (4–11%) was evaluated by modifying the track-quality selections and by comparing the probability to prolong the TPC tracks to the ITS hits in data and simulation. To estimate the uncertainty on the PID selection efficiency, the nσ distributions for "pure" samples of pions, kaons, and protons were compared in data and MC, and found to be compatible [29]. Besides the analysis was repeated without PID selection, the resulting corrected yields were compatible with those obtained with the PID selection and no systematic uncertainty was assigned. The uncertainty on the selection efficiency (5–8%) originates from imperfections in description in the MC simulation of the topological variables used for preselections and in the BDT. It was estimated by comparing the corrected yields obtained by repeating the analysis with different D^0-meson topological preselections, as well as the selection on the BDT response, resulting in a significant modification of the efficiency. The systematic uncertainty on the $f_{\text{non-prompt}}$ fraction estimation (2–8%) was evaluated by changing the selections defining the sets used for the χ^2 minimisation calculation. The systematic effect on the efficiency due to a possible difference between the real and simulated D^0-meson p_T distributions (1–8%) was evaluated by reweighting the D^0-meson spectrum in the simulation so to match alternative p_T distributions. The contributions of the different sources were summed in quadrature to obtain the total systematic uncertainty (8–19%).

5 Results

The p_T-differential production yields of non-prompt D^0 mesons in the 0–10% and 30–50% centrality classes in Pb-Pb collisions at $\sqrt{s_{NN}} = 5.02\,\text{TeV}$ for $p_T > 1\,\text{GeV}/c$ are shown in the top panel of figure 2. They are compared to the corresponding pp reference cross section [102] multiplied by $\langle T_{AA}\rangle$ in the given centrality range. For $24 < p_T < 36\,\text{GeV}/c$, the pp reference cross section was extrapolated exploiting FONLL predictions in a similar way to that used in refs. [22, 27]. To get an indication of the typical B-meson p_T probed in the non-prompt D^0 p_T intervals, a simulation was done in which B^0 and B^+ mesons were generated according to the p_T-differential spectrum expected from FONLL [97, 98] and decayed with the PYTHIA 8.243 event generator. As an example, for non-prompt D^0 with $1 < p_T < 2$ ($10 < p_T < 12$) GeV/c the parent B-meson p_T distribution has a median of $p_T \approx 3.3$ (18.2) GeV/c and an RMS of about 1.9 (6.2) GeV/c. Thus, the measured spectra probe B mesons down to p_T lower than the B meson mass.

The R_{AA} of non-prompt D^0 mesons as a function of p_T is shown in the middle and bottom panels of figure 2 for the 0–10% and 30–50% centrality classes, respectively. The uncertainty on the R_{AA} normalisation results from the quadratic sum of the pp normalisation uncertainty, the uncertainty on $\langle T_{AA}\rangle$, and the centrality interval definition un-

JHEP12(2022)126

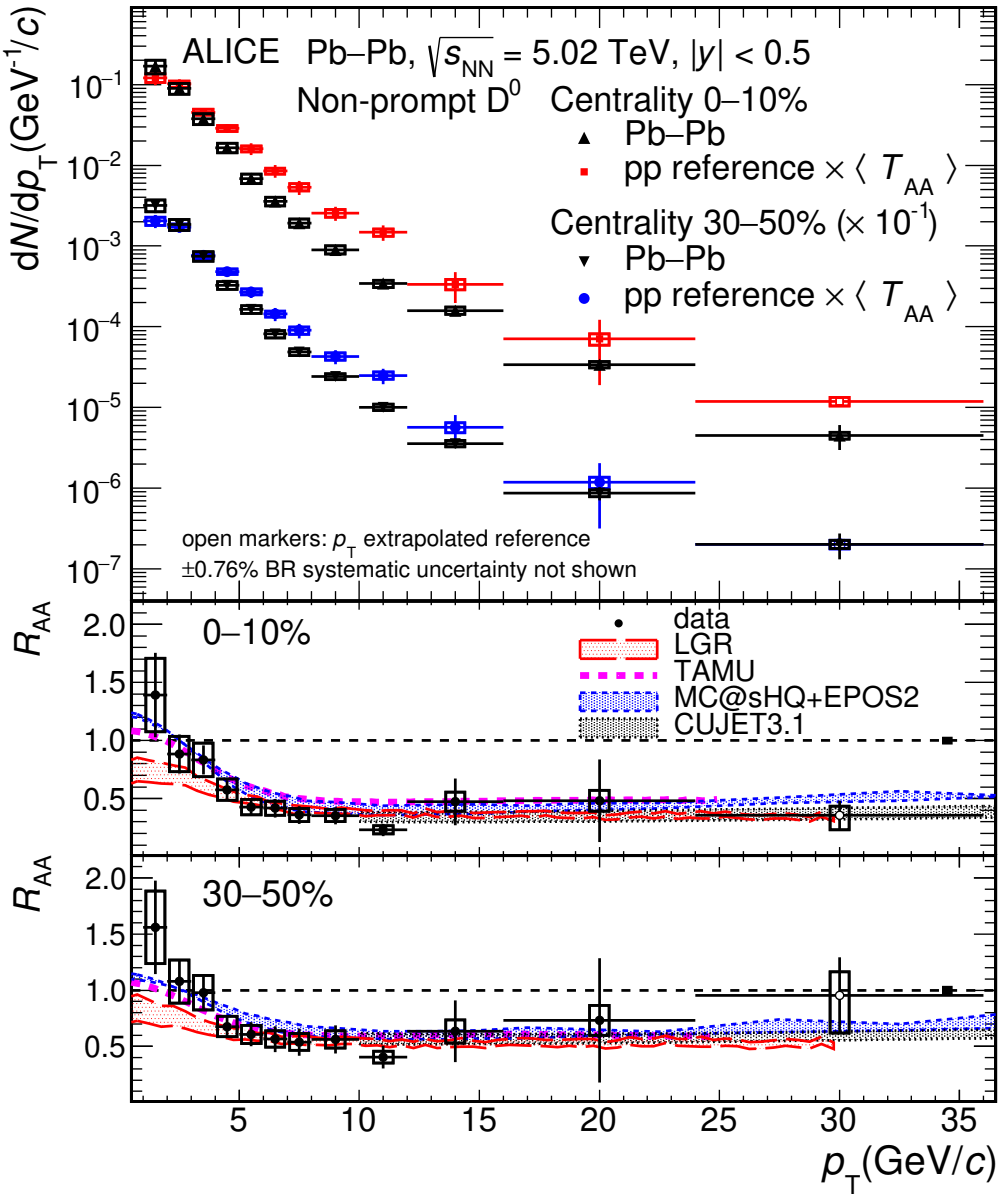

Figure 2. Top panel: non-prompt D^0-meson p_T-differential production yields in Pb-Pb collisions at $\sqrt{s_{NN}} = 5.02$ TeV in the 0–10% and 30–50% centrality classes. The pp reference spectra, $\langle T_{AA} \rangle \times d\sigma_{pp}/dp_T$ [20, 102], are also shown. Middle and bottom panels: p_T-differential R_{AA} in the 0–10% (middle) and 30–50% (bottom) centrality classes, compared with model predictions [72, 73, 85, 103, 104]. Open markers indicate the points for which the pp reference is extrapolated (see text). Vertical bars, empty boxes, and the shaded box around $R_{AA} = 1$ represent the statistical, systematic, and normalisation uncertainty, respectively.

JHEP12(2022)126

certainty [27]. The BR uncertainty is cancelled in the ratio, while all other sources are propagated as uncorrelated. For p_{T} larger than about 5 GeV/c, the R_{AA} does not change significantly with p_{T} and it shows a suppression of the yields by a factor about 3 (2) in the 0–10% (30–50%) centrality class with respect to the pp reference scaled by $\langle T_{\mathrm{AA}}\rangle$. At lower p_{T}, the R_{AA} increases with decreasing p_{T}. Within a 1σ uncertainty, it is compatible with unity in the interval $1 < p_{\mathrm{T}} < 3\,\mathrm{GeV}/c$ ($1 < p_{\mathrm{T}} < 4\,\mathrm{GeV}/c$) in the 0–10% (30–50%) centrality class. Values above unity are slightly favoured by data in the range $1 < p_{\mathrm{T}} < 2\,\mathrm{GeV}/c$. The measured R_{AA} is compared with predictions from various models, namely MC@sHQ+EPOS2 [73], LGR [85, 103], TAMU [72], and CUJET3.1 [104]. In the TAMU model, the heavy-quark interactions with the medium are described by elastic collisions only. The LGR, MC@sHQ+EPOS2, and CUJET3.1 models include both radiative and collisional processes. The contribution of hadronisation via quark recombination, in addition to independent fragmentation, is considered in the TAMU, MC@sHQ+EPOS2, and LGR models. All predictions describe the data within uncertainties in both centrality classes, except for TAMU, which tends to underestimate the suppression in the interval $5 < p_{\mathrm{T}} < 12\,\mathrm{GeV}/c$ in central collisions. This comparison suggests that both radiative and collisional processes are important for beauty quark in-medium energy loss at LHC energies.

Shadowing and a modification of hadronisation can also modify the p_{T}-integrated yield of the final-state beauty hadrons, which is not influenced by the quark energy loss, and cause p_{T}-integrated R_{AA} ($p_{\mathrm{T}} > 0$) to deviate from unity. In order to test this, an extrapolation of the measured spectrum to the intervals $0 < p_{\mathrm{T}} < 1\,\mathrm{GeV}/c$ was performed. The total non-prompt D^0-meson yields in $|y| < 0.5$ for $p_{\mathrm{T}} > 0$ in the 0–10% and 30–50% centrality classes are calculated by adding to the "visible yields", computed by integrating in p_{T} the p_{T}-differential yields measured for $p_{\mathrm{T}} > 1\,\mathrm{GeV}/c$, an estimate of the yield in $0 < p_{\mathrm{T}} < 1\,\mathrm{GeV}/c$ reckoned as

$$\left.\frac{\mathrm{d}N}{\mathrm{d}p_{\mathrm{T}}}\right|^{\text{non-prompt}}_{\text{Pb-Pb, extrap.}}(0 < p_{\mathrm{T}} < 1\,\mathrm{GeV}/c) = R^{\text{prompt}}_{\text{AA, measured}} \times \left.\frac{R^{\text{non-prompt}}_{\mathrm{AA}}}{R^{\text{prompt}}_{\mathrm{AA}}}\right|_{\text{model}} \times \langle T_{\mathrm{AA}}\rangle \times \left.\frac{\mathrm{d}\sigma}{\mathrm{d}p_{\mathrm{T}}}\right|^{\text{non-prompt}}_{\text{pp, extrap.}}. \tag{5.1}$$

In the above equation, all terms on the right side are evaluated in $0 < p_{\mathrm{T}} < 1\,\mathrm{GeV}/c$. The value of the non-prompt D^0 cross section in pp collisions at $\sqrt{s} = 5.02\,\mathrm{TeV}$, $\mathrm{d}\sigma/\mathrm{d}p_{\mathrm{T}}$, is retrieved from ref. [102] (tables 3 and 4) by scaling the cross section measured in $1 < p_{\mathrm{T}} < 24\,\mathrm{GeV}/c$ by $1 - \alpha = 0.28^{+0.01}_{-0.04}$, where α represents the ratio of the cross section for $1 < p_{\mathrm{T}} < 24\,\mathrm{GeV}/c$ to $p_{\mathrm{T}} > 0$ calculated using FONLL predictions [97, 98]. The contribution of non-prompt D^0 with $p_{\mathrm{T}} > 24\,\mathrm{GeV}/c$ to the total yield is below 0.1% and significantly smaller than the uncertainty on the estimate of the yield in $0 < p_{\mathrm{T}} < 1\,\mathrm{GeV}/c$, described later. Therefore, a correction to avoid the double counting of the contribution of the yield in the interval $24 < p_{\mathrm{T}} < 36\,\mathrm{GeV}/c$, which is already accounted for in the visible Pb-Pb yield, as well as a specific extrapolation for $p_{\mathrm{T}} > 36\,\mathrm{GeV}/c$ were not considered necessary. In eq. (5.1) the pp cross section is multiplied by the nuclear overlap function $\langle T_{\mathrm{AA}}\rangle$ for the considered centrality interval and by an estimate of the non-prompt D^0-meson R_{AA} obtained as the product of the measured prompt D^0-meson R_{AA} [29] and an

JHEP12(2022)126

assumption for the "double R_{AA} ratio" $R_{\mathrm{AA}}^{\text{non-prompt}}/R_{\mathrm{AA}}^{\text{prompt}}$. For the latter, the p_{T} shape of the prediction of the LGR model [85, 103], which describes the measured double R_{AA} ratio for $p_{\mathrm{T}} > 1\,\mathrm{GeV}/c$ within uncertainties, is exploited. The model prediction is parametrised with a 5th-order polynomial function, which is then used to fit the data in the interval $1 < p_{\mathrm{T}} < 12\,\mathrm{GeV}/c$, leaving an overall scaling factor as the only free parameter of the fit. The value of the function at $p_{\mathrm{T}} = 0.5\,\mathrm{GeV}/c$ is assumed as the estimate of the double R_{AA} ratio in $0 < p_{\mathrm{T}} < 1\,\mathrm{GeV}/c$. The rescaling of the LGR prediction is performed mainly to avoid a potential unphysical discontinuity in the double R_{AA} ratio between the measured and extrapolated ranges. It was verified that the original value of LGR at $p_{\mathrm{T}} = 0.5\,\mathrm{GeV}/c$ gives a value of the p_{T}-integrated yield that is compatible with that obtained with the default procedure within 1σ of the extrapolation uncertainty. The latter is obtained by summing in quadrature i) the statistical and systematic uncertainties on $R_{\mathrm{AA,\ measured}}^{\text{prompt}}$, ii) the statistical and systematic uncertainties on $\mathrm{d}\sigma/\mathrm{d}p_{\mathrm{T}}$, which include the uncertainty on the extrapolation factor α as well as the uncertainties on the visible cross section, and iii) the uncertainty on the double R_{AA} ratio. The latter is determined by the sum in quadrature of the statistical uncertainty on the scaling factor of the LGR-based parametrisation of the double R_{AA} ratio and the modeling uncertainty, which is determined from the envelope of the values obtained by reparametrising the double R_{AA} ratio using the lower and upper predictions of LGR, as well as the TAMU [72] model, which also reproduces the data within uncertainties for $p_{\mathrm{T}} > 1\,\mathrm{GeV}/c$. Moreover, also the values evaluated at $p_{\mathrm{T}} = 0.63\,\mathrm{GeV}/c$ rather than $p_{\mathrm{T}} = 0.5\,\mathrm{GeV}/c$ are considered, with the former value representing the average p_{T} of non-prompt D^0 mesons with $0 < p_{\mathrm{T}} < 1\,\mathrm{GeV}/c$ according to a simulation performed by decaying with PYTHIA 8.243 [96] B mesons generated according to the expected p_{T} spectrum of FONLL. The envelope spreads around the value of the double R_{AA} ratio obtained with the default LGR prediction covering a relative variation of about $^{+19\%}_{-23\%}$ ($^{+62\%}_{-37\%}$) in the 0–10% (30–50%) centrality class.

The systematic uncertainties on the visible yield are determined by summing those of the p_{T}-differential yields assuming that all uncertainty sources provide uncertainties correlated with p_{T}, with the exception of the yield-extraction uncertainties, which are assumed as uncorrelated with p_{T} and summed in quadrature. The statistical uncertainty is calculated by summing in quadrature those on the p_{T}-differential yields.

The uncertainties on the visible yield and on the estimate of the yield in $0 < p_{\mathrm{T}} < 1\,\mathrm{GeV}/c$ obtained with the procedure described above, are considered as uncorrelated in the sum performed to calculate the yield in $p_{\mathrm{T}} > 0$. The partial correlation induced by constraining the parametrisation of the double R_{AA} ratio to the data is assumed to be negligible. Thanks to the low-p_{T} reach of the measurement, the visible yields represent about 77% and 82% of the estimated total yields in the 0–10% and 30–50% centrality classes, respectively, and the extrapolation uncertainties are 10% and 13%, respectively.

The non-prompt D^0 yields estimated in the 0–10% and 30–50% centrality classes with the above procedure are divided by the non-prompt D^0 pp cross section for $p_{\mathrm{T}} > 0$ [102] scaled by the $\langle T_{\mathrm{AA}} \rangle$ value specific to each centrality class to get the non-prompt R_{AA} for $p_{\mathrm{T}} > 0$. The uncertainty on the R_{AA} is calculated taking properly into account that the α factor and the visible pp cross section are used for determining both the Pb-Pb and pp

JHEP12(2022)126

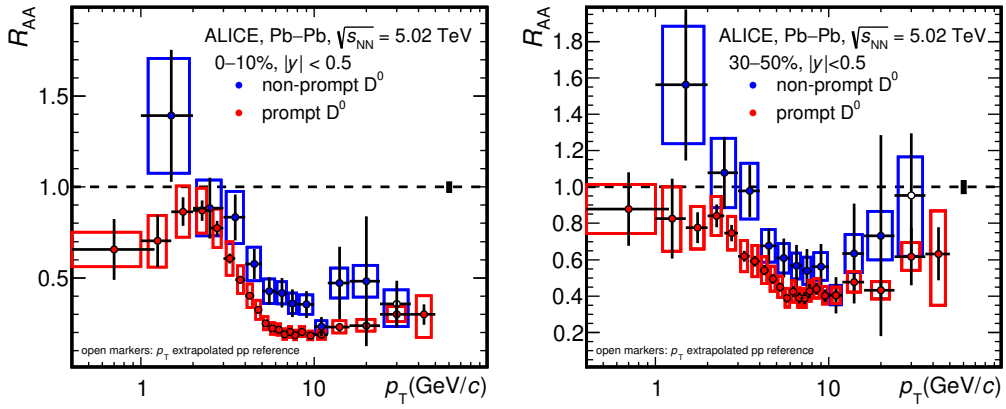

Figure 3. Nuclear modification factor (R_{AA}) of non-prompt D^0 mesons in the centrality classes 0–10% (left) and 30–50% (right), compared with the R_{AA} of prompt D^0 mesons [29]. The statistical and total systematic uncertainties are shown as error bars and boxes, respectively. The normalisation uncertainties are shown as boxes around unity.

p_{T}-integrated yields. All other sources of uncertainties are considered uncorrelated between the Pb-Pb and pp yields, with exception of that on the BR, which cancels in the ratio.

The resulting total yields per unity of rapidity are 0.428 ± 0.033 (stat.) $\pm$ 0.050 (syst.)$^{+0.037}_{-0.042}$ (extr.) $\pm\, 0.004$ (BR) and 0.079 ± 0.007 (stat.) $\pm\, 0.009$ (syst.)$^{+0.010}_{-0.007}$ (extr.) $\pm$ 0.001 (BR) in the 0–10% and 30–50% centrality classes, respectively. The R_{AA} for $p_{\mathrm{T}} > 0$ is 1.00 ± 0.10 (stat.) $\pm\, 0.13$ (syst.)$^{+0.08}_{-0.09}$ (extr.) $\pm\, 0.02$ (norm.) in the 0–10% and 1.10 ± 0.12 (stat.) $\pm\, 0.15$ (syst.)$^{+0.14}_{-0.09}$ (extr.) $\pm\, 0.03$ (norm.) in the 30–50% centrality class. Considering the statistical and systematic uncertainties, in both centrality classes, the R_{AA} is compatible with unity within less than 1σ and with the prompt D^0-meson p_{T}-integrated R_{AA} [29] within less than 1.5σ.

Figure 3 shows the R_{AA} of non-prompt D^0 mesons in Pb-Pb collisions at $\sqrt{s_{\mathrm{NN}}} =$ 5.02 TeV, compared with the R_{AA} of prompt D^0 mesons [29] in the 0–10% and 30–50% centrality classes. The non-prompt D^0 R_{AA} is systematically higher than the prompt D^0 one for $p_{\mathrm{T}} > 5\,\mathrm{GeV}/c$ in both 0–10% and 30–50% centrality classes, indicating that non-prompt D^0 mesons are less suppressed than prompt D^0 ones and supporting the expectation that beauty quarks lose less energy than charm quarks because of their larger mass.

The $R_{\mathrm{AA}}^{\text{non-prompt}}/R_{\mathrm{AA}}^{\text{prompt}}$ ratio as a function of p_{T} is presented in figure 4 for the 0–10% central Pb-Pb collisions. In the computation of the ratio, the tracking-efficiency and normalisation uncertainties get cancelled. All other sources of systematic uncertainties were propagated as uncorrelated. As visible in the top panel, the p_{T} trends of the $R_{\mathrm{AA}}^{\text{non-prompt}}/R_{\mathrm{AA}}^{\text{prompt}}$ ratio predicted by the LGR, MC@sHQ+EPOS2, and TAMU models at low p_{T} are similar. They have a minimum close to unity in $2 < p_{\mathrm{T}} < 3\,\mathrm{GeV}/c$ and increase towards lower and higher p_{T}, a trend resembling the data one, which however cannot be assessed in a conclusive way given the uncertainties. For $p_{\mathrm{T}} > 5\,\mathrm{GeV}/c$ the measured values do not vary significantly with p_{T}: their average is 1.70 ± 0.18, thus about 3.9σ above unity. All considered models, including CUJET3.1, predict a mild decrease of the ratio for $p_{\mathrm{T}} \gtrsim 10\,\mathrm{GeV}/c$, which is steeper for CUJET3.1 and TAMU, with the latter predicting a maximum at $p_{\mathrm{T}} \sim 5\,\mathrm{GeV}/c$. All models describe the data within uncertainties.

JHEP12(2022)126

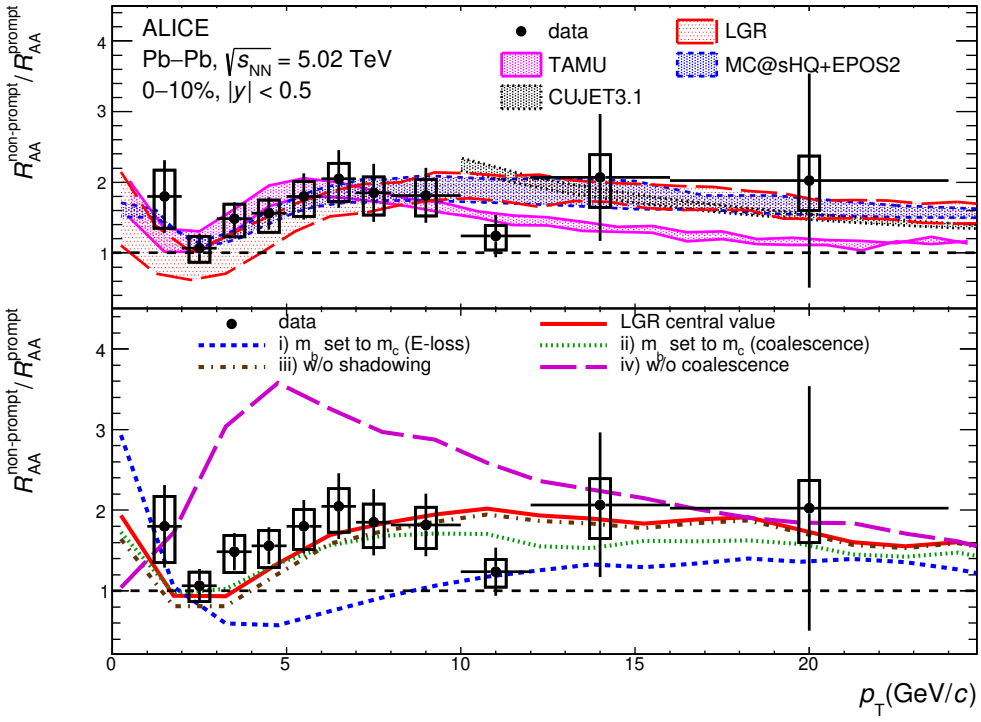

Figure 4. Non-prompt to prompt [29] D^0-meson R_{AA} ratio as a function of p_T in the 0–10% central Pb-Pb collisions at $\sqrt{s_{NN}} = 5.02$ TeV, compared to model predictions [72, 73, 85, 103, 104] (top), and to different modifications of LGR calculations (bottom).

In the bottom panel of figure 4, the ratio of the non-prompt to prompt D^0-meson R_{AA} is compared with predictions from the default LGR calculations as well as four different modifications of the LGR model: i) using the charm-quark mass in the calculation of the beauty-quark energy loss, ii) using the charm-quark mass in beauty-quark coalescence, iii) excluding shadowing effects for both charm and beauty quarks, and iv) excluding quark coalescence in both charm and beauty-quark hadronisation. The configurations (ii) and (iii) give results similar to the default LGR calculation and can describe the data well. The effect of shadowing is relevant mainly at low p_T and it largely gets cancelled in the R_{AA} ratio [103]. The usage of the charm-quark mass in beauty coalescence reduces the R_{AA} ratio at high p_T, as expected from the reduced coalescence probability, while it has a marginal effect for $p_T \lesssim 7\,\mathrm{GeV}/c$. By removing the quark recombination in hadronisation of both charm and beauty quarks (case iv), the R_{AA} ratio is instead significantly enhanced for $p_T > 1\,\mathrm{GeV}/c$ and reduced at lower p_T. This suggests that the minimum of the R_{AA} ratio at $p_T \sim 2.5\,\mathrm{GeV}/c$ in the default LGR calculations is mainly due to the formation of prompt D mesons via charm-quark coalescence. In this process, D mesons acquire a momentum larger than that of the parent charm quarks, causing a hardening of the prompt D^0-meson p_T spectrum. By replacing the beauty-quark mass with that of the charm quark in the beauty-quark energy loss (case i), the R_{AA} ratio reduces significantly for $p_T > 2.5\,\mathrm{GeV}/c$ and becomes lower than unity in $2 < p_T < 8\,\mathrm{GeV}/c$, which is inconsistent with data. This supports the interpretation that the mass-dependence of quark in-medium energy-loss causes the R_{AA} ratio to be significantly larger than unity at intermediate p_T.

JHEP12(2022)126

6 Conclusions

In summary, the R_{AA} of non-prompt D^0 mesons from beauty-hadron decays was measured at midrapidity, $|y| < 0.5$, for $1 < p_{\mathrm{T}} < 36\,\mathrm{GeV}/c$ in Pb-Pb collisions at $\sqrt{s_{\mathrm{NN}}} = 5.02\,\mathrm{TeV}$ in the 0–10% and 30–50% centrality classes. While p_{T}-integrated R_{AA} ($p_{\mathrm{T}} > 0$), which is not directly sensitive to partonic energy loss, is compatible with unity, a significant suppression up to a factor of about three is observed for $p_{\mathrm{T}} > 5\,\mathrm{GeV}/c$ in the 0–10% central Pb-Pb collisions. The data are described by models that include both collisional and radiative processes in the calculation of beauty quark in-medium energy loss and quark recombination as a hadronisation mechanism. The non-prompt D^0-meson R_{AA} is significantly larger than the prompt one. Models that describe their ratio as a function of p_{T} encode a quark-mass dependence of energy loss, both at high p_{T}, where beauty quarks lose less energy than charm quarks via radiative processes, and at low p_{T}, a region in which collisional processes are more relevant and the interaction of heavy quarks with the medium can be described as a diffusion process.

Acknowledgments

The ALICE collaboration would like to thank all its engineers and technicians for their invaluable contributions to the construction of the experiment and the CERN accelerator teams for the outstanding performance of the LHC complex. The ALICE collaboration gratefully acknowledges the resources and support provided by all Grid centres and the Worldwide LHC Computing Grid (WLCG) collaboration. The ALICE collaboration acknowledges the following funding agencies for their support in building and running the ALICE detector: A.I. Alikhanyan National Science Laboratory (Yerevan Physics Institute) Foundation (ANSL), State Committee of Science and World Federation of Scientists (WFS), Armenia; Austrian Academy of Sciences, Austrian Science Fund (FWF): [M 2467-N36] and Nationalstiftung für Forschung, Technologie und Entwicklung, Austria; Ministry of Communications and High Technologies, National Nuclear Research Center, Azerbaijan; Conselho Nacional de Desenvolvimento Científico e Tecnológico (CNPq), Financiadora de Estudos e Projetos (Finep), Fundação de Amparo à Pesquisa do Estado de São Paulo (FAPESP) and Universidade Federal do Rio Grande do Sul (UFRGS), Brazil; Ministry of Education of China (MOEC), Ministry of Science & Technology of China (MSTC) and National Natural Science Foundation of China (NSFC), China; Ministry of Science and Education and Croatian Science Foundation, Croatia; Centro de Aplicaciones Tecnológicas y Desarrollo Nuclear (CEADEN), Cubaenergía, Cuba; Ministry of Education, Youth and Sports of the Czech Republic, Czech Republic; The Danish Council for Independent Research | Natural Sciences, the VILLUM FONDEN and Danish National Research Foundation (DNRF), Denmark; Helsinki Institute of Physics (HIP), Finland; Commissariat à l'Energie Atomique (CEA) and Institut National de Physique Nucléaire et de Physique des Particules (IN2P3) and Centre National de la Recherche Scientifique (CNRS), France; Bundesministerium für Bildung und Forschung (BMBF) and GSI Helmholtzzentrum für Schwerionenforschung GmbH, Germany; General Secretariat for Research and Technol-

JHEP12(2022)126

ogy, Ministry of Education, Research and Religions, Greece; National Research, Development and Innovation Office, Hungary; Department of Atomic Energy Government of India (DAE), Department of Science and Technology, Government of India (DST), University Grants Commission, Government of India (UGC) and Council of Scientific and Industrial Research (CSIR), India; Indonesian Institute of Science, Indonesia; Istituto Nazionale di Fisica Nucleare (INFN), Italy; Japanese Ministry of Education, Culture, Sports, Science and Technology (MEXT) and Japan Society for the Promotion of Science (JSPS) KAKENHI, Japan; Consejo Nacional de Ciencia (CONACYT) y Tecnología, through Fondo de Cooperación Internacional en Ciencia y Tecnología (FONCICYT) and Dirección General de Asuntos del Personal Academico (DGAPA), Mexico; Nederlandse Organisatie voor Wetenschappelijk Onderzoek (NWO), The Netherlands; The Research Council of Norway, Norway; Commission on Science and Technology for Sustainable Development in the South (COMSATS), Pakistan; Pontificia Universidad Católica del Perú, Peru; Ministry of Education and Science, National Science Centre and WUT ID-UB, Poland; Korea Institute of Science and Technology Information and National Research Foundation of Korea (NRF), Republic of Korea; Ministry of Education and Scientific Research, Institute of Atomic Physics, Ministry of Research and Innovation and Institute of Atomic Physics and University Politehnica of Bucharest, Romania; Joint Institute for Nuclear Research (JINR), Ministry of Education and Science of the Russian Federation, National Research Centre Kurchatov Institute, Russian Science Foundation and Russian Foundation for Basic Research, Russia; Ministry of Education, Science, Research and Sport of the Slovak Republic, Slovakia; National Research Foundation of South Africa, South Africa; Swedish Research Council (VR) and Knut & Alice Wallenberg Foundation (KAW), Sweden; European Organization for Nuclear Research, Switzerland; Suranaree University of Technology (SUT), National Science and Technology Development Agency (NSDTA), Suranaree University of Technology (SUT), Thailand Science Research and Innovation (TSRI) and National Science, Research and Innovation Fund (NSRF), Thailand; Turkish Energy, Nuclear and Mineral Research Agency (TENMAK), Turkey; National Academy of Sciences of Ukraine, Ukraine; Science and Technology Facilities Council (STFC), United Kingdom; National Science Foundation of the United States of America (NSF) and United States Department of Energy, Office of Nuclear Physics (DOE NP), United States of America.

Open Access. This article is distributed under the terms of the Creative Commons Attribution License (CC-BY 4.0), which permits any use, distribution and reproduction in any medium, provided the original author(s) and source are credited. SCOAP^3 supports the goals of the International Year of Basic Sciences for Sustainable Development.

References

[1] NA50 collaboration, *Evidence for deconfinement of quarks and gluons from the J/ψ suppression pattern measured in Pb+Pb collisions at the CERN SPS*, *Phys. Lett. B* **477** (2000) 28 [INSPIRE].

[2] WA97 collaboration, *Strangeness enhancement at mid-rapidity in Pb Pb collisions at 158 A GeV/c*, *Phys. Lett. B* **449** (1999) 401 [INSPIRE].

JHEP12(2022)126

[3] BRAHMS collaboration, *Quark gluon plasma and color glass condensate at RHIC? The Perspective from the BRAHMS experiment*, Nucl. Phys. A **757** (2005) 1 [nucl-ex/0410020] [INSPIRE].

[4] PHENIX collaboration, *Formation of dense partonic matter in relativistic nucleus-nucleus collisions at RHIC: Experimental evaluation by the PHENIX collaboration*, Nucl. Phys. A **757** (2005) 184 [nucl-ex/0410003] [INSPIRE].

[5] PHOBOS collaboration, *The PHOBOS perspective on discoveries at RHIC*, Nucl. Phys. A **757** (2005) 28 [nucl-ex/0410022] [INSPIRE].

[6] STAR collaboration, *Experimental and theoretical challenges in the search for the quark gluon plasma: The STAR collaboration's critical assessment of the evidence from RHIC collisions*, Nucl. Phys. A **757** (2005) 102 [nucl-ex/0501009] [INSPIRE].

[7] Y. Schutz and U.A. Wiedemann eds., *Proceedings of the 22nd International Conference on Ultra-Relativistic Nucleus-Nucleus Collisions (Quark Matter 2011)*, Annecy, France, 23–28 May 2011, J. Phys. G **38** (2011) 120301 [INSPIRE].

[8] G. Roland, K. Safarik and P. Steinberg, *Heavy-ion collisions at the LHC*, Prog. Part. Nucl. Phys. **77** (2014) 70 [INSPIRE].

[9] P. Braun-Munzinger, V. Koch, T. Schäfer and J. Stachel, *Properties of hot and dense matter from relativistic heavy ion collisions*, Phys. Rept. **621** (2016) 76 [arXiv:1510.00442] [INSPIRE].

[10] F. Karsch, *Lattice simulations of the thermodynamics of strongly interacting elementary particles and the exploration of new phases of matter in relativistic heavy ion collisions*, J. Phys. Conf. Ser. **46** (2006) 122 [hep-lat/0608003] [INSPIRE].

[11] Wuppertal-Budapest collaboration, *Is there still any T_c mystery in lattice QCD? Results with physical masses in the continuum limit. Part II*, JHEP **09** (2010) 073 [arXiv:1005.3508] [INSPIRE].

[12] S. Borsanyi, Z. Fodor, C. Hoelbling, S.D. Katz, S. Krieg and K.K. Szabo, *Full result for the QCD equation of state with $2+1$ flavors*, Phys. Lett. B **730** (2014) 99 [arXiv:1309.5258] [INSPIRE].

[13] A. Bazavov et al., *The chiral and deconfinement aspects of the QCD transition*, Phys. Rev. D **85** (2012) 054503 [arXiv:1111.1710] [INSPIRE].

[14] M. Gyulassy and M. Plumer, *Jet Quenching in Dense Matter*, Phys. Lett. B **243** (1990) 432 [INSPIRE].

[15] R. Baier, Y.L. Dokshitzer, A.H. Mueller, S. Peigné and D. Schiff, *Radiative energy loss and $p_\perp$ broadening of high-energy partons in nuclei*, Nucl. Phys. B **484** (1997) 265 [hep-ph/9608322] [INSPIRE].

[16] M.H. Thoma and M. Gyulassy, *Quark Damping and Energy Loss in the High Temperature QCD*, Nucl. Phys. B **351** (1991) 491 [INSPIRE].

[17] E. Braaten and M.H. Thoma, *Energy loss of a heavy fermion in a hot plasma*, Phys. Rev. D **44** (1991) 1298 [INSPIRE].

[18] E. Braaten and M.H. Thoma, *Energy loss of a heavy quark in the quark-gluon plasma*, Phys. Rev. D **44** (1991) R2625.

[19] R.J. Glauber and G. Matthiae, *High-energy scattering of protons by nuclei*, Nucl. Phys. B **21** (1970) 135 [INSPIRE].

JHEP12(2022)126

[20] ALICE collaboration, *Centrality determination in heavy ion collisions*, ALICE-PUBLIC-2018-011 (2018) [INSPIRE].

[21] ALICE collaboration, *Measurements of low-p_T electrons from semileptonic heavy-flavour hadron decays at mid-rapidity in pp and Pb-Pb collisions at $\sqrt{s_{\rm NN}} = 2.76$ TeV*, JHEP **10** (2018) 061 [arXiv:1805.04379] [INSPIRE].

[22] ALICE collaboration, *Measurement of D^0, D^+, D^{*+} and D_s^+ production in Pb-Pb collisions at $\sqrt{s_{\rm NN}} = 5.02$ TeV*, JHEP **10** (2018) 174 [arXiv:1804.09083] [INSPIRE].

[23] ALICE collaboration, *Suppression of high transverse momentum D mesons in central Pb-Pb collisions at $\sqrt{s_{\rm NN}} = 2.76$ TeV*, JHEP **09** (2012) 112 [arXiv:1203.2160] [INSPIRE].

[24] ALICE collaboration, *Production of muons from heavy flavour decays at forward rapidity in pp and Pb-Pb collisions at $\sqrt{s_{\rm NN}} = 2.76$ TeV*, Phys. Rev. Lett. **109** (2012) 112301 [arXiv:1205.6443] [INSPIRE].

[25] CMS collaboration, *Nuclear modification factor of D^0 mesons in PbPb collisions at $\sqrt{s_{\rm NN}} = 5.02$ TeV*, Phys. Lett. B **782** (2018) 474 [arXiv:1708.04962] [INSPIRE].

[26] ALICE collaboration, *Measurement of D_s^+ production and nuclear modification factor in Pb-Pb collisions at $\sqrt{s_{\rm NN}} = 2.76$ TeV*, JHEP **03** (2016) 082 [arXiv:1509.07287] [INSPIRE].

[27] ALICE collaboration, *Transverse momentum dependence of D-meson production in Pb-Pb collisions at $\sqrt{s_{\rm NN}} = 2.76$ TeV*, JHEP **03** (2016) 081 [arXiv:1509.06888] [INSPIRE].

[28] ALICE collaboration, *Measurement of electrons from beauty-hadron decays in p-Pb collisions at $\sqrt{s_{\rm NN}} = 5.02$ TeV and Pb-Pb collisions at $\sqrt{s_{\rm NN}} = 2.76$ TeV*, JHEP **07** (2017) 052 [arXiv:1609.03898] [INSPIRE].

[29] ALICE collaboration, *Prompt D^0, D^+, and D^{*+} production in Pb-Pb collisions at $\sqrt{s_{\rm NN}} = 5.02$ TeV*, JHEP **01** (2022) 174 [arXiv:2110.09420] [INSPIRE].

[30] ALICE collaboration, *Measurement of prompt D_s^+-meson production and azimuthal anisotropy in Pb-Pb collisions at $\sqrt{s_{\rm NN}} = 5.02$ TeV*, Phys. Lett. B **827** (2022) 136986 [arXiv:2110.10006] [INSPIRE].

[31] STAR collaboration, *Observation of D^0 Meson Nuclear Modifications in Au+Au Collisions at $\sqrt{s_{\rm NN}} = 200$ GeV*, Phys. Rev. Lett. **113** (2014) 142301 [arXiv:1404.6185] [INSPIRE].

[32] STAR collaboration, *Transverse momentum and centrality dependence of high-p_T non-photonic electron suppression in Au+Au collisions at $\sqrt{s_{\rm NN}} = 200$ GeV*, Phys. Rev. Lett. **98** (2007) 192301 [nucl-ex/0607012] [INSPIRE].

[33] PHENIX collaboration, *Nuclear-Modification Factor for Open-Heavy-Flavor Production at Forward Rapidity in Cu+Cu Collisions at $\sqrt{s_{\rm NN}} = 200$ GeV*, Phys. Rev. C **86** (2012) 024909 [arXiv:1204.0754] [INSPIRE].

[34] PHENIX collaboration, *Heavy Quark Production in p+p and Energy Loss and Flow of Heavy Quarks in Au+Au Collisions at $\sqrt{s_{\rm NN}} = 200$ GeV*, Phys. Rev. C **84** (2011) 044905 [arXiv:1005.1627] [INSPIRE].

[35] PHENIX collaboration, *Nuclear modification of electron spectra and implications for heavy quark energy loss in Au+Au collisions at $\sqrt{s_{\rm NN}} = 200$ GeV*, Phys. Rev. Lett. **96** (2006) 032301 [nucl-ex/0510047] [INSPIRE].

[36] CMS collaboration, *Study of B Meson Production in p+Pb Collisions at $\sqrt{s_{\rm NN}} = 5.02$ TeV Using Exclusive Hadronic Decays*, Phys. Rev. Lett. **116** (2016) 032301 [arXiv:1508.06678] [INSPIRE].

JHEP12(2022)126

[37] CMS collaboration, *Suppression of non-prompt J/ψ, prompt J/ψ, and $\Upsilon(1S)$ in PbPb collisions at $\sqrt{s_{\rm NN}} = 2.76$ TeV*, *JHEP* **05** (2012) 063 [arXiv:1201.5069] [INSPIRE].

[38] CMS collaboration, *Suppression and azimuthal anisotropy of prompt and nonprompt J/ψ production in PbPb collisions at $\sqrt{s_{\rm NN}} = 2.76$ TeV*, *Eur. Phys. J. C* **77** (2017) 252 [arXiv:1610.00613] [INSPIRE].

[39] CMS collaboration, *Studies of Beauty Suppression via Nonprompt D^0 Mesons in Pb-Pb Collisions at $Q^2 = 4\,\mathrm{GeV}^2$*, *Phys. Rev. Lett.* **123** (2019) 022001 [arXiv:1810.11102] [INSPIRE].

[40] CMS collaboration, *Measurement of the $B^\pm$ Meson Nuclear Modification Factor in Pb-Pb Collisions at $\sqrt{s_{\rm NN}} = 5.02$ TeV*, *Phys. Rev. Lett.* **119** (2017) 152301 [arXiv:1705.04727] [INSPIRE].

[41] ATLAS collaboration, *Measurement of the suppression and azimuthal anisotropy of muons from heavy-flavor decays in Pb+Pb collisions at $\sqrt{s_{\rm NN}} = 2.76$ TeV with the ATLAS detector*, *Phys. Rev. C* **98** (2018) 044905 [arXiv:1805.05220] [INSPIRE].

[42] ATLAS collaboration, *Prompt and non-prompt J/ψ and $\psi(2S)$ suppression at high transverse momentum in 5.02 TeV Pb+Pb collisions with the ATLAS experiment*, *Eur. Phys. J. C* **78** (2018) 762 [arXiv:1805.04077] [INSPIRE].

[43] ALICE collaboration, *Centrality dependence of the nuclear modification factor of charged pions, kaons, and protons in Pb-Pb collisions at $\sqrt{s_{\rm NN}} = 2.76$ TeV*, *Phys. Rev. C* **93** (2016) 034913 [arXiv:1506.07287] [INSPIRE].

[44] CMS collaboration, *Measurement of prompt and nonprompt charmonium suppression in PbPb collisions at 5.02 TeV*, *Eur. Phys. J. C* **78** (2018) 509 [arXiv:1712.08959] [INSPIRE].

[45] ALICE collaboration, *Centrality dependence of high-p_T D meson suppression in Pb-Pb collisions at $\sqrt{s_{\rm NN}} = 2.76$ TeV*, *JHEP* **11** (2015) 205 [INSPIRE].

[46] Y.L. Dokshitzer and D.E. Kharzeev, *Heavy quark colorimetry of QCD matter*, *Phys. Lett. B* **519** (2001) 199 [hep-ph/0106202] [INSPIRE].

[47] N. Armesto, C.A. Salgado and U.A. Wiedemann, *Medium induced gluon radiation off massive quarks fills the dead cone*, *Phys. Rev. D* **69** (2004) 114003 [hep-ph/0312106] [INSPIRE].

[48] B.-W. Zhang, E. Wang and X.-N. Wang, *Heavy quark energy loss in nuclear medium*, *Phys. Rev. Lett.* **93** (2004) 072301 [nucl-th/0309040] [INSPIRE].

[49] M. Djordjevic and M. Gyulassy, *Heavy quark radiative energy loss in QCD matter*, *Nucl. Phys. A* **733** (2004) 265 [nucl-th/0310076] [INSPIRE].

[50] ALICE collaboration, *Direct observation of the dead-cone effect in quantum chromodynamics*, *Nature* **605** (2022) 440 [arXiv:2106.05713] [INSPIRE].

[51] STAR collaboration, *Evidence of Mass Ordering of Charm and Bottom Quark Energy Loss in Au+Au Collisions at RHIC*, arXiv:2111.14615 [INSPIRE].

[52] PHENIX collaboration, *Single electron yields from semileptonic charm and bottom hadron decays in Au+Au collisions at $\sqrt{s_{\rm NN}} = 200$ GeV*, *Phys. Rev. C* **93** (2016) 034904 [arXiv:1509.04662] [INSPIRE].

[53] ATLAS collaboration, *Measurement of the nuclear modification factor for muons from charm and bottom hadrons in Pb+Pb collisions at 5.02 TeV with the ATLAS detector*, *Phys. Lett. B* **829** (2022) 137077 [arXiv:2109.00411] [INSPIRE].

JHEP12(2022)126

[54] ALICE collaboration, *Measurement of electrons from beauty-hadron decays in p-Pb collisions at* $\sqrt{s_{\rm NN}} = 5.02$ *TeV and Pb-Pb collisions at* $\sqrt{s_{\rm NN}} = 2.76$ *TeV*, *JHEP* **07** (2017) 052 [arXiv:1609.03898] [INSPIRE].

[55] ALICE collaboration, *Inclusive, prompt and non-prompt J/ψ production at mid-rapidity in Pb-Pb collisions at* $\sqrt{s_{\rm NN}} = 2.76$ *TeV*, *JHEP* **07** (2015) 051 [arXiv:1504.07151] [INSPIRE].

[56] S. Batsouli, S. Kelly, M. Gyulassy and J.L. Nagle, *Does the charm flow at RHIC?*, *Phys. Lett. B* **557** (2003) 26 [nucl-th/0212068] [INSPIRE].

[57] V. Greco, C.M. Ko and R. Rapp, *Quark coalescence for charmed mesons in ultrarelativistic heavy ion collisions*, *Phys. Lett. B* **595** (2004) 202 [nucl-th/0312100] [INSPIRE].

[58] G.D. Moore and D. Teaney, *How much do heavy quarks thermalize in a heavy ion collision?*, *Phys. Rev. C* **71** (2005) 064904 [hep-ph/0412346] [INSPIRE].

[59] P. Petreczky and D. Teaney, *Heavy quark diffusion from the lattice*, *Phys. Rev. D* **73** (2006) 014508 [hep-ph/0507318] [INSPIRE].

[60] ALICE collaboration, *Measurement of prompt* D^0, D^+, D^{*+}, *and* D_S^+ *production in p-Pb collisions at* $\sqrt{s_{\rm NN}} = 5.02$ *TeV*, *JHEP* **12** (2019) 092 [arXiv:1906.03425] [INSPIRE].

[61] ALICE collaboration, *Prompt and non-prompt J/ψ production and nuclear modification at mid-rapidity in p-Pb collisions at* $\sqrt{s_{\rm NN}} = 5.02$ *TeV*, *Eur. Phys. J. C* **78** (2018) 466 [arXiv:1802.00765] [INSPIRE].

[62] LHCb collaboration, *Prompt and nonprompt J/ψ production and nuclear modification in pPb collisions at* $\sqrt{s_{\rm NN}} = 8.16$ *TeV*, *Phys. Lett. B* **774** (2017) 159 [arXiv:1706.07122] [INSPIRE].

[63] LHCb collaboration, *Study of prompt* D^0 *meson production in pPb collisions at* $\sqrt{s_{\rm NN}} = 5$ *TeV*, *JHEP* **10** (2017) 090 [arXiv:1707.02750] [INSPIRE].

[64] LHCb collaboration, *Measurement of* B^+, B^0 *and* Λ_b^0 *production in pPb collisions at* $\sqrt{s_{\rm NN}} = 8.16$ *TeV*, *Phys. Rev. D* **99** (2019) 052011 [arXiv:1902.05599] [INSPIRE].

[65] A. Kusina, J.-P. Lansberg, I. Schienbein and H.-S. Shao, *Gluon Shadowing in Heavy-Flavor Production at the LHC*, *Phys. Rev. Lett.* **121** (2018) 052004 [arXiv:1712.07024] [INSPIRE].

[66] ATLAS collaboration, *Measurement of differential J/ψ production cross sections and forward-backward ratios in p+Pb collisions with the ATLAS detector*, *Phys. Rev. C* **92** (2015) 034904 [arXiv:1505.08141] [INSPIRE].

[67] CMS collaboration, *Study of B Meson Production in p+Pb Collisions at* $\sqrt{s_{\rm NN}} = 5.02$ *TeV Using Exclusive Hadronic Decays*, *Phys. Rev. Lett.* **116** (2016) 032301 [arXiv:1508.06678] [INSPIRE].

[68] A. Andronic, P. Braun-Munzinger, K. Redlich and J. Stachel, *Statistical hadronization of charm in heavy ion collisions at SPS, RHIC and LHC*, *Phys. Lett. B* **571** (2003) 36 [nucl-th/0303036] [INSPIRE].

[69] R.J. Fries, B. Muller, C. Nonaka and S.A. Bass, *Hadronization in heavy ion collisions: Recombination and fragmentation of partons*, *Phys. Rev. Lett.* **90** (2003) 202303 [nucl-th/0301087] [INSPIRE].

[70] L. Ravagli and R. Rapp, *Quark Coalescence based on a Transport Equation*, *Phys. Lett. B* **655** (2007) 126 [arXiv:0705.0021] [INSPIRE].

[71] CMS collaboration, *Measurement of* B_s^0 *meson production in pp and PbPb collisions at* $\sqrt{s_{\rm NN}} = 5.02$ *TeV*, *Phys. Lett. B* **796** (2019) 168 [arXiv:1810.03022] [INSPIRE].

JHEP12(2022)126

[72] M. He, R.J. Fries and R. Rapp, *Heavy Flavor at the Large Hadron Collider in a Strong Coupling Approach*, Phys. Lett. B **735** (2014) 445 [arXiv:1401.3817] [INSPIRE].

[73] M. Nahrgang, J. Aichelin, P.B. Gossiaux and K. Werner, *Influence of hadronic bound states above T_c on heavy-quark observables in Pb+Pb collisions at at the CERN Large Hadron Collider*, Phys. Rev. C **89** (2014) 014905 [arXiv:1305.6544] [INSPIRE].

[74] S. Li, C. Wang, R. Wan and J. Liao, *Probing the transport properties of Quark-Gluon Plasma via heavy-flavor Boltzmann and Langevin dynamics*, Phys. Rev. C **99** (2019) 054909 [arXiv:1901.04600] [INSPIRE].

[75] A. Beraudo, A. De Pace, M. Monteno, M. Nardi and F. Prino, *Heavy flavors in heavy-ion collisions: quenching, flow and correlations*, Eur. Phys. J. C **75** (2015) 121 [arXiv:1410.6082] [INSPIRE].

[76] A. Beraudo, A. De Pace, M. Monteno, M. Nardi and F. Prino, *Event-shape engineering and heavy-flavour observables in relativistic heavy-ion collisions*, Eur. Phys. J. C **79** (2019) 494 [arXiv:1812.08337] [INSPIRE].

[77] T. Song, H. Berrehrah, D. Cabrera, W. Cassing and E. Bratkovskaya, *Charm production in Pb+Pb collisions at energies available at the CERN Large Hadron Collider*, Phys. Rev. C **93** (2016) 034906 [arXiv:1512.00891] [INSPIRE].

[78] S. Cao, T. Luo, G.-Y. Qin and X.-N. Wang, *Linearized Boltzmann transport model for jet propagation in the quark-gluon plasma: Heavy quark evolution*, Phys. Rev. C **94** (2016) 014909 [arXiv:1605.06447] [INSPIRE].

[79] S. Cao, T. Luo, G.-Y. Qin and X.-N. Wang, *Heavy and light flavor jet quenching at RHIC and LHC energies*, Phys. Lett. B **777** (2018) 255 [arXiv:1703.00822] [INSPIRE].

[80] W. Ke, Y. Xu and S.A. Bass, *Linearized Boltzmann-Langevin model for heavy quark transport in hot and dense QCD matter*, Phys. Rev. C **98** (2018) 064901 [arXiv:1806.08848] [INSPIRE].

[81] W. Ke, Y. Xu and S.A. Bass, *Modified Boltzmann approach for modeling the splitting vertices induced by the hot QCD medium in the deep Landau-Pomeranchuk-Migdal region*, Phys. Rev. C **100** (2019) 064911 [arXiv:1810.08177] [INSPIRE].

[82] C.A.G. Prado et al., *Event-by-event correlations between soft hadrons and D^0 mesons in 5.02 TeV PbPb collisions at the CERN Large Hadron Collider*, Phys. Rev. C **96** (2017) 064903 [arXiv:1611.02965] [INSPIRE].

[83] R. Katz, C.A.G. Prado, J. Noronha-Hostler, J. Noronha and A.A.P. Suaide, *Sensitivity study with a D and B mesons modular simulation code of heavy flavor R_{AA} and azimuthal anisotropies based on beam energy, initial conditions, hadronization, and suppression mechanisms*, Phys. Rev. C **102** (2020) 024906 [arXiv:1906.10768] [INSPIRE].

[84] A. Beraudo et al., *Extraction of Heavy-Flavor Transport Coefficients in QCD Matter*, Nucl. Phys. A **979** (2018) 21 [arXiv:1803.03824] [INSPIRE].

[85] S. Li and J. Liao, *Data-driven extraction of heavy quark diffusion in quark-gluon plasma*, Eur. Phys. J. C **80** (2020) 671 [arXiv:1912.08965] [INSPIRE].

[86] R. Rapp, *Heavy-Flavor Transport and Hadronization in the QGP*, PoS **BEAUTY2020** (2021) 033 [INSPIRE].

[87] A. Francis, O. Kaczmarek, M. Laine, T. Neuhaus and H. Ohno, *Nonperturbative estimate of the heavy quark momentum diffusion coefficient*, Phys. Rev. D **92** (2015) 116003 [arXiv:1508.04543] [INSPIRE].

JHEP12(2022)126

[88] S.Y.F. Liu and R. Rapp, *Spectral and transport properties of quark-gluon plasma in a nonperturbative approach*, *Eur. Phys. J. A* **56** (2020) 44 [arXiv:1612.09138] [INSPIRE].

[89] F. Riek and R. Rapp, *Quarkonia and Heavy-Quark Relaxation Times in the Quark-Gluon Plasma*, *Phys. Rev. C* **82** (2010) 035201 [arXiv:1005.0769] [INSPIRE].

[90] ALICE collaboration, *The ALICE experiment at the CERN LHC*, *JINST* **3** (2008) S08002 [INSPIRE].

[91] ALICE collaboration, *Performance of the ALICE Experiment at the CERN LHC*, *Int. J. Mod. Phys. A* **29** (2014) 1430044 [arXiv:1402.4476] [INSPIRE].

[92] J. Alme et al., *The ALICE TPC, a large 3-dimensional tracking device with fast readout for ultra-high multiplicity events*, *Nucl. Instrum. Meth. A* **622** (2010) 316 [arXiv:1001.1950] [INSPIRE].

[93] ALICE collaboration, *Alignment of the ALICE Inner Tracking System with cosmic-ray tracks*, *JINST* **5** (2010) P03003 [arXiv:1001.0502] [INSPIRE].

[94] A. Akindinov et al., *Performance of the ALICE Time-Of-Flight detector at the LHC*, *Eur. Phys. J. Plus* **128** (2013) 44 [INSPIRE].

[95] X.-N. Wang and M. Gyulassy, *HIJING: A Monte Carlo model for multiple jet production in pp, pA and AA collisions*, *Phys. Rev. D* **44** (1991) 3501 [INSPIRE].

[96] T. Sjöstrand et al., *An introduction to PYTHIA 8.2*, *Comput. Phys. Commun.* **191** (2015) 159 [arXiv:1410.3012] [INSPIRE].

[97] M. Cacciari, M. Greco and P. Nason, *The p_{T} spectrum in heavy flavor hadroproduction*, *JHEP* **05** (1998) 007 [hep-ph/9803400] [INSPIRE].

[98] M. Cacciari, S. Frixione and P. Nason, *The p_{T} spectrum in heavy flavor photoproduction*, *JHEP* **03** (2001) 006 [hep-ph/0102134] [INSPIRE].

[99] R. Brun et al., *GEANT Detector Description and Simulation Tool*, CERN-W-5013 (1994) [INSPIRE].

[100] Particle Data collaboration, *Review of Particle Physics*, *Prog. Theor. Exp. Phys.* **2020** (2020) 083C01 [INSPIRE].

[101] A. Hocker et al., *TMVA — Toolkit for Multivariate Data Analysis*, physics/0703039 [INSPIRE].

[102] ALICE collaboration, *Measurement of beauty and charm production in pp collisions at $\sqrt{s} = 5.02$ TeV via non-prompt and prompt D mesons*, *JHEP* **05** (2021) 220 [arXiv:2102.13601] [INSPIRE].

[103] S. Li, W. Xiong and R. Wan, *Relativistic Langevin dynamics: charm versus beauty*, *Eur. Phys. J. C* **80** (2020) 1113 [arXiv:2012.02489] [INSPIRE].

[104] S. Shi, J. Liao and M. Gyulassy, *Global constraints from RHIC and LHC on transport properties of QCD fluids in CUJET/CIBJET framework*, *Chin. Phys. C* **43** (2019) 044101 [arXiv:1808.05461] [INSPIRE].

JHEP12(2022)126

The ALICE collaboration

S. Acharya,[143] D. Adamová,[97] A. Adler,[75] J. Adolfsson,[82] G. Aglieri Rinella,[35] M. Agnello,[31] N. Agrawal,[55] Z. Ahammed,[143] S. Ahmad,[17] S.U. Ahn,[77] I. Ahuja,[39] Z. Akbar,[52] A. Akindinov,[94] M. Al-Turany,[109] S.N. Alam,[17] D. Aleksandrov,[90] B. Alessandro,[60] H.M. Alfanda,[7] R. Alfaro Molina,[72] B. Ali,[17] Y. Ali,[15] A. Alici,[26] N. Alizadehvandchali,[126] A. Alkin,[35] J. Alme,[22] G. Alocco,[56] T. Alt,[69] I. Altsybeev,[114] M.N. Anaam,[7] C. Andrei,[49] A. Andronic,[146] V. Anguelov,[106] F. Antinori,[58] P. Antonioli,[55] C. Anuj,[17] N. Apadula,[81] L. Aphecetche,[116] H. Appelshäuser,[69] S. Arcelli,[26] R. Arnaldi,[60] I.C. Arsene,[21] M. Arslandok,[148] A. Augustinus,[35] R. Averbeck,[109] S. Aziz,[79] M.D. Azmi,[17] A. Badalà,[57] Y.W. Baek,[42] X. Bai,[130,109] R. Bailhache,[69] Y. Bailung,[51] R. Bala,[103] A. Balbino,[31] A. Baldisseri,[140] B. Balis,[2] D. Banerjee,[4] Z. Banoo,[103] R. Barbera,[27] L. Barioglio,[107] M. Barlou,[86] G.G. Barnaföldi,[147] L.S. Barnby,[96] V. Barret,[137] C. Bartels,[129] K. Barth,[35] E. Bartsch,[69] F. Baruffaldi,[28] N. Bastid,[137] S. Basu,[82] G. Batigne,[116] D. Battistini,[107] B. Batyunya,[76] D. Bauri,[50] J.L. Bazo Alba,[113] I.G. Bearden,[91] C. Beattie,[148] P. Becht,[109] I. Belikov,[139] A.D.C. Bell Hechavarria,[146] F. Bellini,[26] R. Bellwied,[126] S. Belokurova,[114] V. Belyaev,[95] G. Bencedi,[147,70] S. Beole,[25] A. Bercuci,[49] Y. Berdnikov,[100] A. Berdnikova,[106] L. Bergmann,[106] M.G. Besoiu,[68] L. Betev,[35] P.P. Bhaduri,[143] A. Bhasin,[103] I.R. Bhat,[103] M.A. Bhat,[4] B. Bhattacharjee,[43] L. Bianchi,[25] N. Bianchi,[53] J. Bielčík,[38] J. Bielčíková,[97] J. Biernat,[119] A. Bilandzic,[107] G. Biro,[147] S. Biswas,[4] J.T. Blair,[120] D. Blau,[90,83] M.B. Blidaru,[109] C. Blume,[69] G. Boca,[29,59] F. Bock,[98] A. Bogdanov,[95] S. Boi,[23] J. Bok,[62] L. Boldizsár,[147] A. Bolozdynya,[95] M. Bombara,[39] P.M. Bond,[35] G. Bonomi,[142,59] H. Borel,[140] A. Borissov,[83] H. Bossi,[148] E. Botta,[25] L. Bratrud,[69] P. Braun-Munzinger,[109] M. Bregant,[122] M. Broz,[38] G.E. Bruno,[108,34] M.D. Buckland,[24,129] D. Budnikov,[110] H. Buesching,[69] S. Bufalino,[31] O. Bugnon,[116] P. Buhler,[115] Z. Buthelezi,[73,133] J.B. Butt,[15] A. Bylinkin,[22,128] S.A. Bysiak,[119] M. Cai,[28,7] H. Caines,[148] A. Caliva,[109] E. Calvo Villar,[113] J.M.M. Camacho,[121] R.S. Camacho,[46] P. Camerini,[24] F.D.M. Canedo,[122] M. Carabas,[136] F. Carnesecchi,[35,26] R. Caron,[138,140] J. Castillo Castellanos,[140] F. Catalano,[31] C. Ceballos Sanchez,[76] I. Chakaberia,[81] P. Chakraborty,[50] S. Chandra,[143] S. Chapeland,[35] M. Chartier,[129] S. Chattopadhyay,[143] S. Chattopadhyay,[111] T.G. Chavez,[46] T. Cheng,[7] C. Cheshkov,[138] B. Cheynis,[138] V. Chibante Barroso,[35] D.D. Chinellato,[123] E.S. Chizzali,[107] S. Cho,[62] P. Chochula,[35] P. Christakoglou,[92] C.H. Christensen,[91] P. Christiansen,[82] T. Chujo,[135] C. Cicalo,[56] L. Cifarelli,[26] F. Cindolo,[55] M.R. Ciupek,[109] G. Clai,[II,55] J. Cleymans,[I,125] F. Colamaria,[54] J.S. Colburn,[112] D. Colella,[54,108,34] A. Collu,[81] M. Colocci,[26,35] M. Concas,[III,60] G. Conesa Balbastre,[80] Z. Conesa del Valle,[79] G. Contin,[24] J.G. Contreras,[38] M.L. Coquet,[140] T.M. Cormier,[98] P. Cortese,[32] M.R. Cosentino,[124] F. Costa,[35] S. Costanza,[29,59] P. Crochet,[137] R. Cruz-Torres,[81] E. Cuautle,[70] P. Cui,[7] L. Cunqueiro,[98] A. Dainese,[58] M.C. Danisch,[106] A. Danu,[68] P. Das,[88] P. Das,[4] S. Das,[4] S. Dash,[50] A. De Caro,[30] G. de Cataldo,[54] L. De Cilladi,[25] J. de Cuveland,[40] A. De Falco,[23] D. De Gruttola,[30] N. De Marco,[60] C. De Martin,[24] S. De Pasquale,[30] S. Deb,[51] H.F. Degenhardt,[122] K.R. Deja,[144] R. Del Grande,[107] L. Dello Stritto,[30] W. Deng,[7] P. Dhankher,[20] D. Di Bari,[34] A. Di Mauro,[35] R.A. Diaz,[76,8] T. Dietel,[125] Y. Ding,[138,7] R. Divià,[35] D.U. Dixit,[20] Ø. Djuvsland,[22] U. Dmitrieva,[64] A. Dobrin,[68] B. Dönigus,[69] A.K. Dubey,[143] A. Dubla,[109,92] S. Dudi,[102] P. Dupieux,[137] M. Durkac,[118] N. Dzalaiova,[14] T.M. Eder,[146] R.J. Ehlers,[98] V.N. Eikeland,[22] F. Eisenhut,[69] D. Elia,[54] B. Erazmus,[116] F. Ercolessi,[26] E. Eremenko,[97] F. Erhardt,[101] A. Erokhin,[114] M.R. Ersdal,[22] B. Espagnon,[79] G. Eulisse,[35] D. Evans,[112] S. Evdokimov,[93] L. Fabbietti,[107] M. Faggin,[28] J. Faivre,[80] F. Fan,[7] W. Fan,[81] A. Fantoni,[53] M. Fasel,[98] P. Fecchio,[31] A. Feliciello,[60] G. Feofilov,[114]

JHEP12(2022)126

A. Fernández Téllez,[46] A. Ferrero,[140] A. Ferretti,[25] V.J.G. Feuillard,[106] J. Figiel,[119] V. Filova,[38] D. Finogeev,[64] F.M. Fionda,[56] G. Fiorenza,[35] F. Flor,[126] A.N. Flores,[120] S. Foertsch,[73] S. Fokin,[90] E. Fragiacomo,[61] E. Frajna,[147] A. Francisco,[137] U. Fuchs,[35] N. Funicello,[30] C. Furget,[80] A. Furs,[64] J.J. Gaardhøje,[91] M. Gagliardi,[25] A.M. Gago,[113] A. Gal,[139] C.D. Galvan,[121] P. Ganoti,[86] C. Garabatos,[109] J.R.A. Garcia,[46] E. Garcia-Solis,[10] K. Garg,[116] C. Gargiulo,[35] A. Garibli,[89] K. Garner,[146] P. Gasik,[109] E.F. Gauger,[120] A. Gautam,[128] M.B. Gay Ducati,[71] M. Germain,[116] S.K. Ghosh,[4] M. Giacalone,[26] P. Gianotti,[53] P. Giubellino,[109,60] P. Giubilato,[28] A.M.C. Glaenzer,[140] P. Glässel,[106] E. Glimos,[132] D.J.Q. Goh,[84] V. Gonzalez,[145] L.H. González-Trueba,[72] S. Gorbunov,[40] M. Gorgon,[2] L. Görlich,[119] S. Gotovac,[36] V. Grabski,[72] L.K. Graczykowski,[144] L. Greiner,[81] A. Grelli,[63] C. Grigoras,[35] V. Grigoriev,[95] S. Grigoryan,[76,1] F. Grosa,[35,60] J.F. Grosse-Oetringhaus,[35] R. Grosso,[109] D. Grund,[38] G.G. Guardiano,[123] R. Guernane,[80] M. Guilbaud,[116] K. Gulbrandsen,[91] T. Gunji,[134] W. Guo,[7] A. Gupta,[103] R. Gupta,[103] S.P. Guzman,[46] L. Gyulai,[147] M.K. Habib,[109] C. Hadjidakis,[79] H. Hamagaki,[84] M. Hamid,[7] R. Hannigan,[120] M.R. Haque,[144] A. Harlenderova,[109] J.W. Harris,[148] A. Harton,[10] J.A. Hasenbichler,[35] H. Hassan,[98] D. Hatzifotiadou,[55] P. Hauer,[44] L.B. Havener,[148] S.T. Heckel,[107] E. Hellbär,[109] H. Helstrup,[37] T. Herman,[38] G. Herrera Corral,[9] F. Herrmann,[146] K.F. Hetland,[37] B. Heybeck,[69] H. Hillemanns,[35] C. Hills,[129] B. Hippolyte,[139] B. Hofman,[63] B. Hohlweger,[92] J. Honermann,[146] G.H. Hong,[149] D. Horak,[38] S. Hornung,[109] A. Horzyk,[2] R. Hosokawa,[16] Y. Hou,[7] P. Hristov,[35] C. Hughes,[132] P. Huhn,[69] L.M. Huhta,[127] C.V. Hulse,[79] T.J. Humanic,[99] H. Hushnud,[111] L.A. Husova,[146] A. Hutson,[126] J.P. Iddon,[129] R. Ilkaev,[110] H. Ilyas,[15] M. Inaba,[135] G.M. Innocenti,[35] M. Ippolitov,[90] A. Isakov,[97] T. Isidori,[128] M.S. Islam,[111] M. Ivanov,[109] V. Ivanov,[100] V. Izucheev,[93] M. Jablonski,[2] B. Jacak,[81] N. Jacazio,[35] P.M. Jacobs,[81] S. Jadlovska,[118] J. Jadlovsky,[118] S. Jaelani,[63] C. Jahnke,[123] M.J. Jakubowska,[144] A. Jalotra,[103] M.A. Janik,[144] T. Janson,[75] M. Jercic,[101] O. Jevons,[112] A.A.P. Jimenez,[70] F. Jonas,[98,146] P.G. Jones,[112] J.M. Jowett ,[35,109] J. Jung,[69] M. Jung,[69] A. Junique,[35] A. Jusko,[112] M.J. Kabus,[144] J. Kaewjai,[117] P. Kalinak,[65] A.S. Kalteyer,[109] A. Kalweit,[35] V. Kaplin,[95] A. Karasu Uysal,[78] D. Karatovic,[101] O. Karavichev,[64] T. Karavicheva,[64] P. Karczmarczyk,[144] E. Karpechev,[64] V. Kashyap,[88] A. Kazantsev,[90] U. Kebschull,[75] R. Keidel,[48] D.L.D. Keijdener,[63] M. Keil,[35] B. Ketzer,[44] A.M. Khan,[7] S. Khan,[17] A. Khanzadeev,[100] Y. Kharlov,[93,83] A. Khatun,[17] A. Khuntia,[119] B. Kileng,[37] B. Kim,[18] C. Kim,[18] D.J. Kim,[127] E.J. Kim,[74] J. Kim,[149] J.S. Kim,[42] J. Kim,[106] J. Kim,[74] M. Kim,[106] S. Kim,[19] T. Kim,[149] S. Kirsch,[69] I. Kisel,[40] S. Kiselev,[94] A. Kisiel,[144] J.P. Kitowski,[2] J.L. Klay,[6] J. Klein,[35] S. Klein,[81] C. Klein-Bösing,[146] M. Kleiner,[69] T. Klemenz,[107] A. Kluge,[35] A.G. Knospe,[126] C. Kobdaj,[117] T. Kollegger,[109] A. Kondratyev,[76] N. Kondratyeva,[95] E. Kondratyuk,[93] J. Konig,[69] S.A. Konigstorfer,[107] P.J. Konopka,[35] G. Kornakov,[144] S.D. Koryciak,[2] A. Kotliarov,[97] O. Kovalenko,[87] V. Kovalenko,[114] M. Kowalski,[119] I. Králik,[65] A. Kravčáková,[39] L. Kreis,[109] M. Krivda,[112,65] F. Krizek,[97] K. Krizkova Gajdosova,[38] M. Kroesen,[106] M. Krüger,[69] D.M. Krupova,[38] E. Kryshen,[100] M. Krzewicki,[40] V. Kučera,[35] C. Kuhn,[139] P.G. Kuijer,[92] T. Kumaoka,[135] D. Kumar,[143] L. Kumar,[102] N. Kumar,[102] S. Kundu,[35] P. Kurashvili,[87] A. Kurepin,[64] A.B. Kurepin,[64] A. Kuryakin,[110] S. Kushpil,[97] J. Kvapil,[112] M.J. Kweon,[62] J.Y. Kwon,[62] Y. Kwon,[149] S.L. La Pointe,[40] P. La Rocca,[27] Y.S. Lai,[81] A. Lakrathok,[117] M. Lamanna,[35] R. Langoy,[131] P. Larionov,[35,53] E. Laudi,[35] L. Lautner,[35,107] R. Lavicka,[115,38] T. Lazareva,[114] R. Lea,[142,59] J. Lehrbach,[40] R.C. Lemmon,[96] I. León Monzón,[121] M.M. Lesch,[107] E.D. Lesser,[20] M. Lettrich,[35,107] P. Lévai,[147] X. Li,[11] X.L. Li,[7] J. Lien,[131] R. Lietava,[112] B. Lim,[18] S.H. Lim,[18] V. Lindenstruth,[40] A. Lindner,[49] C. Lippmann,[109] A. Liu,[20] D.H. Liu,[7] J. Liu,[129] I.M. Lofnes,[22] V. Loginov,[95] C. Loizides,[98] P. Loncar,[36] J.A. Lopez,[106] X. Lopez,[137]

JHEP12(2022)126

E. López Torres,[8] J.R. Luhder,[146] M. Lunardon,[28] G. Luparello,[61] Y.G. Ma,[41]
A. Maevskaya,[64] M. Mager,[35] T. Mahmoud,[44] A. Maire,[139] M. Malaev,[100] N.M. Malik,[103]
Q.W. Malik,[21] S.K. Malik,[103] L. Malinina,[IV,76] D. Mal'Kevich,[94] D. Mallick,[88] N. Mallick,[51]
G. Mandaglio,[33,57] V. Manko,[90] F. Manso,[137] V. Manzari,[54] Y. Mao,[7] G.V. Margagliotti,[24]
A. Margotti,[55] A. Marín,[109] C. Markert,[120] M. Marquard,[69] N.A. Martin,[106] P. Martinengo,[35]
J.L. Martinez,[126] M.I. Martínez,[46] G. Martínez García,[116] S. Masciocchi,[109] M. Masera,[25]
A. Masoni,[56] L. Massacrier,[79] A. Mastroserio,[141,54] A.M. Mathis,[107] O. Matonoha,[82]
P.F.T. Matuoka,[122] A. Matyja,[119] C. Mayer,[119] A.L. Mazuecos,[35] F. Mazzaschi,[25]
M. Mazzilli,[35] J.E. Mdhluli,[133] A.F. Mechler,[69] Y. Melikyan,[64] A. Menchaca-Rocha,[72]
E. Meninno,[115,30] A.S. Menon,[126] M. Meres,[14] S. Mhlanga,[125,73] Y. Miake,[135] L. Micheletti,[60]
L.C. Migliorin,[138] D.L. Mihaylov,[107] K. Mikhaylov,[76,94] A.N. Mishra,[147] D. Miśkowiec,[109]
A. Modak,[4] A.P. Mohanty,[63] B. Mohanty,[88] M. Mohisin Khan,[V,17] M.A. Molander,[45]
Z. Moravcova,[91] C. Mordasini,[107] D.A. Moreira De Godoy,[146] I. Morozov,[64] A. Morsch,[35]
T. Mrnjavac,[35] V. Muccifora,[53] E. Mudnic,[36] S. Muhuri,[143] J.D. Mulligan,[81] A. Mulliri,[23]
M.G. Munhoz,[122] R.H. Munzer,[69] H. Murakami,[134] S. Murray,[125] L. Musa,[35] J. Musinsky,[65]
J.W. Myrcha,[144] B. Naik,[133] R. Nair,[87] B.K. Nandi,[50] R. Nania,[55] E. Nappi,[54]
A.F. Nassirpour,[82] A. Nath,[106] C. Nattrass,[132] A. Neagu,[21] A. Negru,[136] L. Nellen,[70]
S.V. Nesbo,[37] G. Neskovic,[40] D. Nesterov,[114] B.S. Nielsen,[91] E.G. Nielsen,[91] S. Nikolaev,[90]
S. Nikulin,[90] V. Nikulin,[100] F. Noferini,[55] S. Noh,[13] P. Nomokonov,[76] J. Norman,[129]
N. Novitzky,[135] P. Nowakowski,[144] A. Nyanin,[90] J. Nystrand,[22] M. Ogino,[84] A. Ohlson,[82]
V.A. Okorokov,[95] J. Oleniacz,[144] A.C. Oliveira Da Silva,[132] M.H. Oliver,[148] A. Onnerstad,[127]
C. Oppedisano,[60] A. Ortiz Velasquez,[70] T. Osako,[47] A. Oskarsson,[82] J. Otwinowski,[119]
M. Oya,[47] K. Oyama,[84] Y. Pachmayer,[106] S. Padhan,[50] D. Pagano,[142,59] G. Paić,[70]
A. Palasciano,[54] S. Panebianco,[140] J. Park,[62] J.E. Parkkila,[127] S.P. Pathak,[126]
R.N. Patra,[103,35] B. Paul,[23] H. Pei,[7] T. Peitzmann,[63] X. Peng,[12,7] L.G. Pereira,[71]
H. Pereira Da Costa,[140] D. Peresunko,[90,83] G.M. Perez,[8] S. Perrin,[140] Y. Pestov,[5]
V. Petráček,[38] V. Petrov,[114] M. Petrovici,[49] R.P. Pezzi,[116,71] S. Piano,[61] M. Pikna,[14]
P. Pillot,[116] O. Pinazza,[55,35] L. Pinsky,[126] C. Pinto,[27] S. Pisano,[53] M. Płoskoń,[81]
M. Planinic,[101] F. Pliquett,[69] M.G. Poghosyan,[98] B. Polichtchouk,[93] S. Politano,[31]
N. Poljak,[101] A. Pop,[49] S. Porteboeuf-Houssais,[137] J. Porter,[81] V. Pozdniakov,[76] S.K. Prasad,[4]
R. Preghenella,[55] F. Prino,[60] C.A. Pruneau,[145] I. Pshenichnov,[64] M. Puccio,[35] S. Qiu,[92]
L. Quaglia,[25] R.E. Quishpe,[126] S. Ragoni,[112] A. Rakotozafindrabe,[140] L. Ramello,[32]
F. Rami,[139] S.A.R. Ramirez,[46] T.A. Rancien,[80] R. Raniwala,[104] S. Raniwala,[104]
S.S. Räsänen,[45] R. Rath,[51] I. Ravasenga,[92] K.F. Read,[98,132] A.R. Redelbach,[40]
K. Redlich,[VI,87] A. Rehman,[22] P. Reichelt,[69] F. Reidt,[35] H.A. Reme-ness,[37] Z. Rescakova,[39]
K. Reygers,[106] A. Riabov,[100] V. Riabov,[100] R. Ricci,[30] T. Richert,[82] M. Richter,[21]
W. Riegler,[35] F. Riggi,[27] C. Ristea,[68] M. Rodríguez Cahuantzi,[46] K. Røed,[21] R. Rogalev,[93]
E. Rogochaya,[76] T.S. Rogoschinski,[69] D. Rohr,[35] D. Röhrich,[22] P.F. Rojas,[46]
S. Rojas Torres,[38] P.S. Rokita,[144] F. Ronchetti,[53] A. Rosano,[33,57] E.D. Rosas,[70] A. Rossi,[58]
A. Roy,[51] P. Roy,[111] S. Roy,[50] N. Rubini,[26] O.V. Rueda,[82] D. Ruggiano,[144] R. Rui,[24]
B. Rumyantsev,[76] P.G. Russek,[2] R. Russo,[92] A. Rustamov,[89] E. Ryabinkin,[90] Y. Ryabov,[100]
A. Rybicki,[119] H. Rytkonen,[127] W. Rzesa,[144] O.A.M. Saarimaki,[45] R. Sadek,[116] S. Sadovsky,[93]
J. Saetre,[22] K. Šafařík,[38] S.K. Saha,[143] S. Saha,[88] B. Sahoo,[50] P. Sahoo,[50] R. Sahoo,[51]
S. Sahoo,[66] D. Sahu,[51] P.K. Sahu,[66] J. Saini,[143] S. Sakai,[135] M.P. Salvan,[109] S. Sambyal,[103]
T.B. Saramela,[122] D. Sarkar,[145] N. Sarkar,[143] P. Sarma,[43] V.M. Sarti,[107] M.H.P. Sas,[148]
J. Schambach,[98] H.S. Scheid,[69] C. Schiaua,[49] R. Schicker,[106] A. Schmah,[106] C. Schmidt,[109]
H.R. Schmidt,[105] M.O. Schmidt,[35,106] M. Schmidt,[105] N.V. Schmidt,[98,69] A.R. Schmier,[132]
R. Schotter,[139] J. Schukraft,[35] K. Schwarz,[109] K. Schweda,[109] G. Scioli,[26] E. Scomparin,[60]

JHEP12(2022)126

J.E. Seger,[16] Y. Sekiguchi,[134] D. Sekihata,[134] I. Selyuzhenkov,[109,95] S. Senyukov,[139] J.J. Seo,[62] D. Serebryakov,[64] L. Šerkšnytė,[107] A. Sevcenco,[68] T.J. Shaba,[73] A. Shabanov,[64] A. Shabetai,[116] R. Shahoyan,[35] W. Shaikh,[111] A. Shangaraev,[93] A. Sharma,[102] D. Sharma,[50] H. Sharma,[119] M. Sharma,[103] N. Sharma,[102] S. Sharma,[103] U. Sharma,[103] A. Shatat,[79] O. Sheibani,[126] K. Shigaki,[47] M. Shimomura,[85] S. Shirinkin,[94] Q. Shou,[41] Y. Sibiriak,[90] S. Siddhanta,[56] T. Siemiarczuk,[87] T.F. Silva,[122] D. Silvermyr,[82] T. Simantathammakul,[117] G. Simonetti,[35] B. Singh,[107] R. Singh,[88] R. Singh,[103] R. Singh,[51] V.K. Singh,[143] V. Singhal,[143] T. Sinha,[111] B. Sitar,[14] M. Sitta,[32] T.B. Skaali,[21] G. Skorodumovs,[106] M. Slupecki,[45] N. Smirnov,[148] R.J.M. Snellings,[63] C. Soncco,[113] J. Song,[126] A. Songmoolnak,[117] F. Soramel,[28] S. Sorensen,[132] I. Sputowska,[119] J. Stachel,[106] I. Stan,[68] P.J. Steffanic,[132] S.F. Stiefelmaier,[106] D. Stocco,[116] I. Storehaug,[21] M.M. Storetvedt,[37] P. Stratmann,[146] S. Strazzi,[26] C.P. Stylianidis,[92] A.A.P. Suaide,[122] C. Suire,[79] M. Sukhanov,[64] M. Suljic,[35] R. Sultanov,[94] V. Sumberia,[103] S. Sumowidagdo,[52] S. Swain,[66] A. Szabo,[14] I. Szarka,[14] U. Tabassam,[15] S.F. Taghavi,[107] G. Taillepied,[109,137] J. Takahashi,[123] G.J. Tambave,[22] S. Tang,[137,7] Z. Tang,[130] J.D. Tapia Takaki,[VII,128] N. Tapus,[136] M.G. Tarzila,[49] A. Tauro,[35] G. Tejeda Muñoz,[46] A. Telesca,[35] L. Terlizzi,[25] C. Terrevoli,[126] G. Tersimonov,[3] S. Thakur,[143] D. Thomas,[120] R. Tieulent,[138] A. Tikhonov,[64] A.R. Timmins,[126] M. Tkacik,[118] A. Toia,[69] N. Topilskaya,[64] M. Toppi,[53] F. Torales-Acosta,[20] T. Tork,[79] A.G. Torres Ramos,[34] A. Trifiró,[33,57] A.S. Triolo,[33] S. Tripathy,[55] T. Tripathy,[50] S. Trogolo,[35] V. Trubnikov,[3] W.H. Trzaska,[127] T.P. Trzcinski,[144] A. Tumkin,[110] R. Turrisi,[58] T.S. Tveter,[21] K. Ullaland,[22] A. Uras,[138] M. Urioni,[59,142] G.L. Usai,[23] M. Vala,[39] N. Valle,[29] S. Vallero,[60] L.V.R. van Doremalen,[63] M. van Leeuwen,[92] R.J.G. van Weelden,[92] P. Vande Vyvre,[35] D. Varga,[147] Z. Varga,[147] M. Varga-Kofarago,[147] M. Vasileiou,[86] A. Vasiliev,[90] O. Vázquez Doce,[53,107] V. Vechernin,[114] A. Velure,[22] E. Vercellin,[25] S. Vergara Limón,[46] L. Vermunt,[63] R. Vértesi,[147] M. Verweij,[63] L. Vickovic,[36] Z. Vilakazi,[133] O. Villalobos Baillie,[112] G. Vino,[54] A. Vinogradov,[90] T. Virgili,[30] V. Vislavicius,[91] A. Vodopyanov,[76] B. Volkel,[35] M.A. Völkl,[106] K. Voloshin,[94] S.A. Voloshin,[145] G. Volpe,[34] B. von Haller,[35] I. Vorobyev,[107] N. Vozniuk,[64] J. Vrláková,[39] B. Wagner,[22] C. Wang,[41] D. Wang,[41] M. Weber,[115] A. Wegrzynek,[35] S.C. Wenzel,[35] J.P. Wessels,[146] S.L. Weyhmiller,[148] J. Wiechula,[69] J. Wikne,[21] G. Wilk,[87] J. Wilkinson,[109] G.A. Willems,[146] B. Windelband,[106] M. Winn,[140] W.E. Witt,[132] J.R. Wright,[120] W. Wu,[41] Y. Wu,[130] R. Xu,[7] A.K. Yadav,[143] S. Yalcin,[78] Y. Yamaguchi,[47] K. Yamakawa,[47] S. Yang,[22] S. Yano,[47] Z. Yin,[7] I.-K. Yoo,[18] J.H. Yoon,[62] S. Yuan,[22] A. Yuncu,[106] V. Zaccolo,[24] C. Zampolli,[35] H.J.C. Zanoli,[63] F. Zanone,[106] N. Zardoshti,[35,112] A. Zarochentsev,[114] P. Závada,[67] N. Zaviyalov,[110] M. Zhalov,[100] B. Zhang,[7] S. Zhang,[41] X. Zhang,[7] Y. Zhang,[130] V. Zherebchevskii,[114] Y. Zhi,[11] N. Zhigareva,[94] D. Zhou,[7] Y. Zhou,[91] J. Zhu,[109,7] Y. Zhu,[7] G. Zinovjev,[I,3] N. Zurlo[142,59]

[I] *Deceased*
[II] *Also at: Italian National Agency for New Technologies, Energy and Sustainable Economic Development (ENEA), Bologna, Italy*
[III] *Also at: Dipartimento DET del Politecnico di Torino, Turin, Italy*
[IV] *Also at: M.V. Lomonosov Moscow State University, D.V. Skobeltsyn Institute of Nuclear, Physics, Moscow, Russia*
[V] *Also at: Department of Applied Physics, Aligarh Muslim University, Aligarh, India*
[VI] *Also at: Institute of Theoretical Physics, University of Wroclaw, Poland*
[VII] *Also at: University of Kansas, Lawrence, Kansas, United States*

[1] *A.I. Alikhanyan National Science Laboratory (Yerevan Physics Institute) Foundation, Yerevan, Armenia*
[2] *AGH University of Science and Technology, Cracow, Poland*

JHEP12(2022)126

[3] *Bogolyubov Institute for Theoretical Physics, National Academy of Sciences of Ukraine, Kiev, Ukraine*
[4] *Bose Institute, Department of Physics and Centre for Astroparticle Physics and Space Science (CAPSS), Kolkata, India*
[5] *Budker Institute for Nuclear Physics, Novosibirsk, Russia*
[6] *California Polytechnic State University, San Luis Obispo, California, United States*
[7] *Central China Normal University, Wuhan, China*
[8] *Centro de Aplicaciones Tecnológicas y Desarrollo Nuclear (CEADEN), Havana, Cuba*
[9] *Centro de Investigación y de Estudios Avanzados (CINVESTAV), Mexico City and Mérida, Mexico*
[10] *Chicago State University, Chicago, Illinois, United States*
[11] *China Institute of Atomic Energy, Beijing, China*
[12] *China University of Geosciences, Wuhan, China*
[13] *Chungbuk National University, Cheongju, Republic of Korea*
[14] *Comenius University Bratislava, Faculty of Mathematics, Physics and Informatics, Bratislava, Slovakia*
[15] *COMSATS University Islamabad, Islamabad, Pakistan*
[16] *Creighton University, Omaha, Nebraska, United States*
[17] *Department of Physics, Aligarh Muslim University, Aligarh, India*
[18] *Department of Physics, Pusan National University, Pusan, Republic of Korea*
[19] *Department of Physics, Sejong University, Seoul, Republic of Korea*
[20] *Department of Physics, University of California, Berkeley, California, United States*
[21] *Department of Physics, University of Oslo, Oslo, Norway*
[22] *Department of Physics and Technology, University of Bergen, Bergen, Norway*
[23] *Dipartimento di Fisica dell'Università and Sezione INFN, Cagliari, Italy*
[24] *Dipartimento di Fisica dell'Università and Sezione INFN, Trieste, Italy*
[25] *Dipartimento di Fisica dell'Università and Sezione INFN, Turin, Italy*
[26] *Dipartimento di Fisica e Astronomia dell'Università and Sezione INFN, Bologna, Italy*
[27] *Dipartimento di Fisica e Astronomia dell'Università and Sezione INFN, Catania, Italy*
[28] *Dipartimento di Fisica e Astronomia dell'Università and Sezione INFN, Padova, Italy*
[29] *Dipartimento di Fisica e Nucleare e Teorica, Università di Pavia, Pavia, Italy*
[30] *Dipartimento di Fisica 'E.R. Caianiello' dell'Università and Gruppo Collegato INFN, Salerno, Italy*
[31] *Dipartimento DISAT del Politecnico and Sezione INFN, Turin, Italy*
[32] *Dipartimento di Scienze e Innovazione Tecnologica dell'Università del Piemonte Orientale and INFN Sezione di Torino, Alessandria, Italy*
[33] *Dipartimento di Scienze MIFT, Università di Messina, Messina, Italy*
[34] *Dipartimento Interateneo di Fisica 'M. Merlin' and Sezione INFN, Bari, Italy*
[35] *European Organization for Nuclear Research (CERN), Geneva, Switzerland*
[36] *Faculty of Electrical Engineering, Mechanical Engineering and Naval Architecture, University of Split, Split, Croatia*
[37] *Faculty of Engineering and Science, Western Norway University of Applied Sciences, Bergen, Norway*
[38] *Faculty of Nuclear Sciences and Physical Engineering, Czech Technical University in Prague, Prague, Czech Republic*
[39] *Faculty of Science, P.J. Šafárik University, Košice, Slovakia*
[40] *Frankfurt Institute for Advanced Studies, Johann Wolfgang Goethe-Universität Frankfurt, Frankfurt, Germany*
[41] *Fudan University, Shanghai, China*
[42] *Gangneung-Wonju National University, Gangneung, Republic of Korea*
[43] *Gauhati University, Department of Physics, Guwahati, India*
[44] *Helmholtz-Institut für Strahlen- und Kernphysik, Rheinische Friedrich-Wilhelms-Universität Bonn, Bonn, Germany*
[45] *Helsinki Institute of Physics (HIP), Helsinki, Finland*

JHEP12(2022)126

[46] *High Energy Physics Group, Universidad Autónoma de Puebla, Puebla, Mexico*
[47] *Hiroshima University, Hiroshima, Japan*
[48] *Hochschule Worms, Zentrum für Technologietransfer und Telekommunikation (ZTT), Worms, Germany*
[49] *Horia Hulubei National Institute of Physics and Nuclear Engineering, Bucharest, Romania*
[50] *Indian Institute of Technology Bombay (IIT), Mumbai, India*
[51] *Indian Institute of Technology Indore, Indore, India*
[52] *Indonesian Institute of Sciences, Jakarta, Indonesia*
[53] *INFN, Laboratori Nazionali di Frascati, Frascati, Italy*
[54] *INFN, Sezione di Bari, Bari, Italy*
[55] *INFN, Sezione di Bologna, Bologna, Italy*
[56] *INFN, Sezione di Cagliari, Cagliari, Italy*
[57] *INFN, Sezione di Catania, Catania, Italy*
[58] *INFN, Sezione di Padova, Padova, Italy*
[59] *INFN, Sezione di Pavia, Pavia, Italy*
[60] *INFN, Sezione di Torino, Turin, Italy*
[61] *INFN, Sezione di Trieste, Trieste, Italy*
[62] *Inha University, Incheon, Republic of Korea*
[63] *Institute for Gravitational and Subatomic Physics (GRASP), Utrecht University/Nikhef, Utrecht, The Netherlands*
[64] *Institute for Nuclear Research, Academy of Sciences, Moscow, Russia*
[65] *Institute of Experimental Physics, Slovak Academy of Sciences, Košice, Slovakia*
[66] *Institute of Physics, Homi Bhabha National Institute, Bhubaneswar, India*
[67] *Institute of Physics of the Czech Academy of Sciences, Prague, Czech Republic*
[68] *Institute of Space Science (ISS), Bucharest, Romania*
[69] *Institut für Kernphysik, Johann Wolfgang Goethe-Universität Frankfurt, Frankfurt, Germany*
[70] *Instituto de Ciencias Nucleares, Universidad Nacional Autónoma de México, Mexico City, Mexico*
[71] *Instituto de Física, Universidade Federal do Rio Grande do Sul (UFRGS), Porto Alegre, Brazil*
[72] *Instituto de Física, Universidad Nacional Autónoma de México, Mexico City, Mexico*
[73] *iThemba LABS, National Research Foundation, Somerset West, South Africa*
[74] *Jeonbuk National University, Jeonju, Republic of Korea*
[75] *Johann-Wolfgang-Goethe Universität Frankfurt Institut für Informatik, Fachbereich Informatik und Mathematik, Frankfurt, Germany*
[76] *Joint Institute for Nuclear Research (JINR), Dubna, Russia*
[77] *Korea Institute of Science and Technology Information, Daejeon, Republic of Korea*
[78] *KTO Karatay University, Konya, Turkey*
[79] *Laboratoire de Physique des 2 Infinis, Irène Joliot-Curie, Orsay, France*
[80] *Laboratoire de Physique Subatomique et de Cosmologie, Université Grenoble-Alpes, CNRS-IN2P3, Grenoble, France*
[81] *Lawrence Berkeley National Laboratory, Berkeley, California, United States*
[82] *Lund University Department of Physics, Division of Particle Physics, Lund, Sweden*
[83] *Moscow Institute for Physics and Technology, Moscow, Russia*
[84] *Nagasaki Institute of Applied Science, Nagasaki, Japan*
[85] *Nara Women's University (NWU), Nara, Japan*
[86] *National and Kapodistrian University of Athens, School of Science, Department of Physics, Athens, Greece*
[87] *National Centre for Nuclear Research, Warsaw, Poland*
[88] *National Institute of Science Education and Research, Homi Bhabha National Institute, Jatni, India*
[89] *National Nuclear Research Center, Baku, Azerbaijan*
[90] *National Research Centre Kurchatov Institute, Moscow, Russia*
[91] *Niels Bohr Institute, University of Copenhagen, Copenhagen, Denmark*
[92] *Nikhef, National institute for subatomic physics, Amsterdam, Netherlands*

JHEP12(2022)126

[93] NRC Kurchatov Institute IHEP, Protvino, Russia
[94] NRC "Kurchatov" Institute - ITEP, Moscow, Russia
[95] NRNU Moscow Engineering Physics Institute, Moscow, Russia
[96] Nuclear Physics Group, STFC Daresbury Laboratory, Daresbury, United Kingdom
[97] Nuclear Physics Institute of the Czech Academy of Sciences, Řež u Prahy, Czech Republic
[98] Oak Ridge National Laboratory, Oak Ridge, Tennessee, United States
[99] Ohio State University, Columbus, Ohio, United States
[100] Petersburg Nuclear Physics Institute, Gatchina, Russia
[101] Physics department, Faculty of science, University of Zagreb, Zagreb, Croatia
[102] Physics Department, Panjab University, Chandigarh, India
[103] Physics Department, University of Jammu, Jammu, India
[104] Physics Department, University of Rajasthan, Jaipur, India
[105] Physikalisches Institut, Eberhard-Karls-Universität Tübingen, Tübingen, Germany
[106] Physikalisches Institut, Ruprecht-Karls-Universität Heidelberg, Heidelberg, Germany
[107] Physik Department, Technische Universität München, Munich, Germany
[108] Politecnico di Bari and Sezione INFN, Bari, Italy
[109] Research Division and ExtreMe Matter Institute EMMI, GSI Helmholtzzentrum für Schwerionenforschung GmbH, Darmstadt, Germany
[110] Russian Federal Nuclear Center (VNIIEF), Sarov, Russia
[111] Saha Institute of Nuclear Physics, Homi Bhabha National Institute, Kolkata, India
[112] School of Physics and Astronomy, University of Birmingham, Birmingham, United Kingdom
[113] Sección Física, Departamento de Ciencias, Pontificia Universidad Católica del Perú, Lima, Peru
[114] St. Petersburg State University, St. Petersburg, Russia
[115] Stefan Meyer Institut für Subatomare Physik (SMI), Vienna, Austria
[116] SUBATECH, IMT Atlantique, Université de Nantes, CNRS-IN2P3, Nantes, France
[117] Suranaree University of Technology, Nakhon Ratchasima, Thailand
[118] Technical University of Košice, Košice, Slovakia
[119] The Henryk Niewodniczanski Institute of Nuclear Physics, Polish Academy of Sciences, Cracow, Poland
[120] The University of Texas at Austin, Austin, Texas, United States
[121] Universidad Autónoma de Sinaloa, Culiacán, Mexico
[122] Universidade de São Paulo (USP), São Paulo, Brazil
[123] Universidade Estadual de Campinas (UNICAMP), Campinas, Brazil
[124] Universidade Federal do ABC, Santo Andre, Brazil
[125] University of Cape Town, Cape Town, South Africa
[126] University of Houston, Houston, Texas, United States
[127] University of Jyväskylä, Jyväskylä, Finland
[128] University of Kansas, Lawrence, Kansas, United States
[129] University of Liverpool, Liverpool, United Kingdom
[130] University of Science and Technology of China, Hefei, China
[131] University of South-Eastern Norway, Tonsberg, Norway
[132] University of Tennessee, Knoxville, Tennessee, United States
[133] University of the Witwatersrand, Johannesburg, South Africa
[134] University of Tokyo, Tokyo, Japan
[135] University of Tsukuba, Tsukuba, Japan
[136] University Politehnica of Bucharest, Bucharest, Romania
[137] Université Clermont Auvergne, CNRS/IN2P3, LPC, Clermont-Ferrand, France
[138] Université de Lyon, CNRS/IN2P3, Institut de Physique des 2 Infinis de Lyon, Lyon, France
[139] Université de Strasbourg, CNRS, IPHC UMR 7178, F-67000 Strasbourg, France, Strasbourg, France
[140] Université Paris-Saclay Centre d'Etudes de Saclay (CEA), IRFU, Départment de Physique Nucléaire (DPhN), Saclay, France
[141] Università degli Studi di Foggia, Foggia, Italy

JHEP12(2022)126

[142] *Università di Brescia, Brescia, Italy*
[143] *Variable Energy Cyclotron Centre, Homi Bhabha National Institute, Kolkata, India*
[144] *Warsaw University of Technology, Warsaw, Poland*
[145] *Wayne State University, Detroit, Michigan, United States*
[146] *Westfälische Wilhelms-Universität Münster, Institut für Kernphysik, Münster, Germany*
[147] *Wigner Research Centre for Physics, Budapest, Hungary*
[148] *Yale University, New Haven, Connecticut, United States*
[149] *Yonsei University, Seoul, Republic of Korea*

JHEP12(2022)126